CHAPTER 3

HEAT TRANSFER

HEAT is energy in transit due to a temperature difference. The thermal energy is transferred from one region to another by three modes of **heat transfer**: conduction, convection, and radiation. Heat transfer is among a group of energy transport phenomena that includes mass transfer (see Chapter 5), momentum transfer or fluid friction (see Chapter 2), and electrical conduction. Transport phenomena have similar rate equations, in which flux is proportional to a potential difference. In heat transfer by conduction and convection, the potential difference is the temperature difference. Heat, mass, and momentum transfer are often considered together because of their similarities and interrelationship in many common physical processes.

This chapter presents the elementary principles of single-phase heat transfer with emphasis on heating, refrigerating, and air conditioning. Boiling and condensation are discussed in Chapter 4. More specific information on heat transfer to or from buildings or refrigerated spaces can be found in Chapters 25 through 31 of this volume and in Chapter 12 of the *ASHRAE Handbook—Refrigeration*. Physical properties of substances can be found in Chapters 18, 22, 24, and 36 of this volume and in Chapter 8 of the *ASHRAE Handbook—Refrigeration*. Heat transfer equipment, including evaporators, condensers, heating and cooling coils, furnaces, and radiators, is covered in the *ASHRAE Handbook—Systems and Equipment*. For further information on heat transfer, see the section on Bibliography.

HEAT TRANSFER PROCESSES

Thermal Conduction. This is the mechanism of heat transfer whereby energy is transported between parts of a continuum by the transfer of kinetic energy between particles or groups of particles at the atomic level. In gases, conduction is caused by elastic collision of molecules; in liquids and electrically nonconducting solids, it is believed to be caused by longitudinal oscillations of the lattice structure. Thermal conduction in metals occurs, like electrical conduction, through the motion of free electrons. Thermal energy transfer occurs in the direction of decreasing temperature, a consequence of the second law of thermodynamics. In solid opaque bodies, thermal conduction is the significant heat transfer mechanism because no net material flows in the process and radiation is not a factor. With flowing fluids, thermal conduction dominates in the region very close to a solid boundary, where the flow is **laminar** and parallel to the surface and where there is no eddy motion.

Thermal Convection. This form of heat transfer involves energy transfer by fluid movement and molecular conduction (Burmeister 1983, Kays and Crawford 1980). Consider heat transfer to a fluid flowing inside a pipe. If the Reynolds number is large enough, three different flow regions exist. Immediately adjacent to the wall is a **laminar sublayer** where heat transfer occurs by thermal conduction; outside the laminar sublayer is a transition region called the **buffer layer**, where both eddy mixing and conduction effects are significant; beyond the buffer layer and extending to the center of the pipe is the **turbulent region**, where the dominant mechanism of transfer is eddy mixing.

In most equipment, the main body of fluid is in turbulent flow, and the laminar layer exists at the solid walls only. In cases of low-velocity flow in small tubes, or with viscous liquids such as glycol (i.e., at low Reynolds numbers), the entire flow may be laminar with no transition or turbulent region.

When fluid currents are produced by external sources (for example, a blower or pump), the solid-to-fluid heat transfer is termed **forced convection**. If the fluid flow is generated internally by nonhomogeneous densities caused by temperature variation, the heat transfer is termed **free convection** or **natural convection**.

Thermal Radiation. In conduction and convection, heat transfer takes place through matter. In thermal radiation, there is a change in energy form from internal energy at the source to electromagnetic energy for transmission, then back to internal energy at the receiver. Whereas conduction and convection heat transfer rates are driven primarily by temperature difference and somewhat by temperature level, radiative heat transfer rates increase rapidly with temperature levels (for the same temperature difference).

Although some generalized heat transfer equations have been mathematically derived from fundamentals, they are usually obtained from correlations of experimental data. Normally, the correlations employ certain dimensionless numbers, shown in Table 1, that are derived from dimensional analysis or analogy.

STEADY-STATE CONDUCTION

For steady-state heat conduction in one dimension, the Fourier law is

$$q = -(kA)\frac{dt}{dx} \tag{1}$$

where

q = heat flow rate, Btu/h
k = thermal conductivity, Btu·ft/h·ft^2·°F
A = cross-sectional area normal to flow, ft^2
dt/dx = temperature gradient, °F/ft

Equation (1) states that the heat flow rate q in the x direction is directly proportional to the temperature gradient dt/dx and the cross-sectional area A normal to the heat flow. The proportionality factor is the thermal conductivity k. The minus sign indicates that the heat flow is positive in the direction of decreasing temperature. Conductivity values are sometimes given in other units, but consistent units must be used in Equation (1).

The preparation of this chapter is assigned to TC 1.3, Heat Transfer and Fluid Flow.

Table 1 Dimensionless Numbers Commonly Used in Heat Transfer

Name	Symbol	Value[a]	Application
Nusselt number	Nu	hD/k, hL/k, $q''D/\Delta tk$, or $q''L/\Delta tk$	Natural or forced convection, boiling or condensing
Reynolds number	Re	GD/μ or $\rho VL/\mu$	Forced convection, boiling or condensing
Prandtl number	Pr	$\mu c_p/k$	Natural or forced convection, boiling or condensing
Stanton number	St	h/Gc_p	Forced convection
Grashof number	Gr	$L^3\rho^2\beta g\Delta t/\mu^2$ or $L^3\rho^2 g\Delta t/T\mu^2$	Natural convection (for ideal gases)
Fourier number	Fo	$\alpha\tau/L^2$	Unsteady-state conduction
Peclet number	Pe	GDc_p/k or Re Pr	Forced convection (small Pr)
Graetz number	Gz	GD^2c_p/kL or Re Pr D/L	Laminar forced convection

[a]A list of the other symbols used in this chapter appears in the section on Symbols.

Equation (1) may be integrated along a path of constant heat flow rate to obtain

$$q = k\left(\frac{A_m}{L_m}\right)\Delta t = \frac{\Delta t}{R} \tag{2}$$

where

A_m = mean cross-sectional area normal to flow, ft^2
L_m = mean length of heat flow path, ft
Δt = overall temperature difference, °F
R = thermal resistance, °F·h/Btu

Thermal resistance R is directly proportional to the mean length L_m of the heat flow path and inversely proportional to the conductivity k and the mean cross-sectional area A_m normal to the flow. Equations for thermal resistances of a few common shapes are given in Table 2. Mathematical solutions to many heat conduction problems are addressed by Carslaw and Jaeger (1959). Complicated problems can be solved by graphical or numerical methods such as described by Croft and Lilley (1977), Adams and Rogers (1973), and Patankar (1980).

Analogy to Electrical Conduction. Equation (2) is analogous to Ohm's law for electrical circuits: thermal current (heat flow) in a **thermal circuit** is directly proportional to the thermal potential (temperature difference) and inversely proportional to the thermal resistance. This electrical-thermal analogy can be used for heat conduction in complex shapes that resist solution by exact analytical means. The thermal circuit concept is also useful for problems involving combined conduction, convection, and radiation.

OVERALL HEAT TRANSFER

In most steady-state heat transfer problems, more than one heat transfer mode is involved. The various heat transfer coefficients may be combined into an overall coefficient so that the total heat transfer can be calculated from the terminal temperatures. The solution to this problem is much simpler if the concept of a thermal circuit is employed.

Local Overall Heat Transfer Coefficient—Resistance Method

Consider heat transfer from one fluid to another by a three-step steady-state process: from a warmer fluid to a solid wall, through the wall, then to a colder fluid. An **overall heat transfer coefficient** U based on the difference between the bulk temperatures $t_1 - t_2$ of the two fluids is defined as follows:

$$q = UA(t_1 - t_2) \tag{3}$$

where A is the surface area. Because Equation (3) is a definition of U, the surface area A on which U is based is arbitrary; it should always be specified in referring to U.

Table 2 Solutions for Some Steady-State Thermal Conduction Problems

System	R in Equation $q = \Delta t/R$
Flat wall or curved wall if curvature is small (wall thickness less than 0.1 of inside diameter) 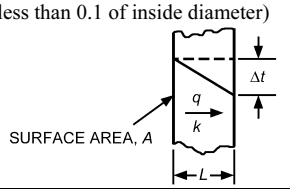	$R = \frac{L}{kA}$
Radial flow through a right circular cylinder 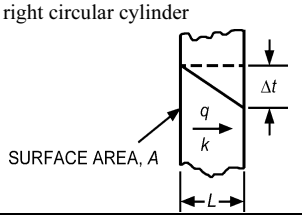	$R = \frac{\ln(r_o/r_i)}{2\pi kL}$
Buried cylinder 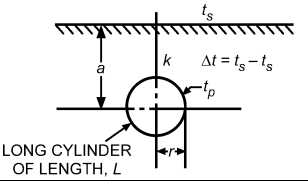	$R = \frac{\ln\left[(a+\sqrt{a^2-r^2})/r\right]}{2\pi kL}$ $= \frac{\cosh^{-1}(a/r)}{2\pi kL}$ $(L \gg 2r)$
Radial flow in a hollow sphere 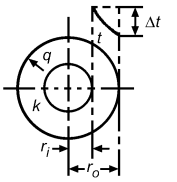	$R = \frac{(1/r_i - 1/r_o)}{4\pi k}$

L, r, a = dimensions, ft
k = thermal conductivity at average material temperature, Btu·ft/h·ft^2·°F
A = surface area, ft^2

The temperature drops across each part of the heat flow path are

$$t_1 - t_{s1} = qR_1$$
$$t_{s1} - t_{s2} = qR_2$$
$$t_{s2} - t_2 = qR_3$$

where t_{s1}, and t_{s2} are the warm and cold surface temperatures of the wall, respectively, and R_1, R_2, and R_3 are the thermal resistances. Because the same quantity of heat flows through each thermal resistance, these equations combined yield the following:

$$\frac{t_1 - t_2}{q} = \frac{1}{UA} = R_1 + R_2 + R_3 \quad (4)$$

As shown above, the equations are analogous to those for electrical circuits; for thermal current flowing through n resistances in *series*, the resistances are additive.

$$R_o = R_1 + R_2 + R_3 + \ldots + R_n \quad (5)$$

Similarly, **conductance** is the reciprocal of resistance, and for heat flow through resistances in *parallel*, the conductances are additive:

$$C = \frac{1}{R_o} = \frac{1}{R_1} + \frac{1}{R_2} + \frac{1}{R_3} + \ldots + \frac{1}{R_n} \quad (6)$$

For convection, the thermal resistance is inversely proportional to the **convection coefficient** h_c and the applicable surface area:

$$R_c = \frac{1}{h_c A} \quad (7)$$

The thermal resistance for radiation is written similarly to that for convection:

$$R_r = \frac{1}{h_r A} \quad (8)$$

The **radiation coefficient** h_r is a function of the temperatures, radiation properties, and geometrical arrangement of the enclosure and the body in question.

Resistance Method Analysis. Analysis by the resistance method can be illustrated by considering heat transfer from air outside to cold water inside an insulated pipe. The temperature gradients and the nature of the resistance analysis are shown in Figure 1.

Because air is sensibly transparent to radiation, some heat transfer occurs by both radiation and convection to the outer insulation surface. The mechanisms act in parallel on the air side. The total transfer then passes through the insulating layer and the pipe wall by thermal conduction, and then by convection and radiation into the cold water stream. (Radiation is not significant on the water side because liquids are sensibly opaque to radiation, although water transmits energy in the visible region.) The contact resistance between the insulation and the pipe wall is assumed negligible.

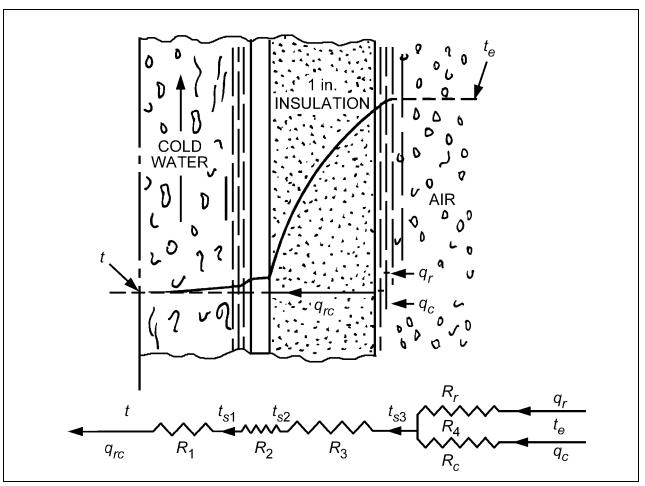

Fig. 1 Thermal Circuit Diagram for Insulated Cold Water Line

The heat transfer rate q_{rc} for a given length L of pipe may be thought of as the sum of the rates q_r and q_c flowing through the parallel resistances R_r and R_c associated with the surface radiation and convection coefficients. The total flow then proceeds through the resistance R_3 offered to thermal conduction by the insulation, through the pipe wall resistance R_2, and into the water stream through the convection resistance R_1. Note the analogy to direct-current electricity. A temperature (potential) drop is required to overcome resistances to the flow of thermal current. The total resistance to heat transfer R_o is the sum of the individual resistances:

$$R_o = R_1 + R_2 + R_3 + R_4 \quad (9)$$

where the resultant parallel resistance R_4 is obtained from

$$\frac{1}{R_4} = \frac{1}{R_r} + \frac{1}{R_c} \quad (10)$$

If the individual resistances can be evaluated, the total resistance can be obtained from this relation. The heat transfer rate for the length of pipe L can be established by

$$q_{rc} = \frac{t_e - t}{R_o} \quad (11)$$

For a unit length of the pipe, the heat transfer rate is

$$\frac{q_{rc}}{L} = \frac{t_e - t}{R_o L} \quad (12)$$

The temperature drop Δt through each individual resistance may then be calculated from the relation:

$$\Delta t_n = R_n q_{rc} \quad (13)$$

where n = 1, 2, and 3.

Mean Temperature Difference

When heat is exchanged between two fluids flowing through a heat exchanger, the local temperature difference Δt varies along the flow path. Heat transfer may be calculated using

$$q = UA\Delta t_m \quad (14)$$

where U is the overall uniform coefficient of heat transfer from fluid to fluid, A is the area associated with the coefficient U, and Δt_m is the appropriate mean temperature difference.

For parallel flow or counterflow exchangers and for any exchanger in which one fluid temperature is substantially constant, the mean temperature difference is

$$\Delta t_m = \frac{\Delta t_1 - \Delta t_2}{\ln(\Delta t_1 / \Delta t_2)} = \frac{\Delta t_1 - \Delta t_2}{2.3 \log(\Delta t_1 / \Delta t_2)} \quad (15)$$

where Δt_1, and Δt_2 are the temperature differences between the fluids at each end of the heat exchanger. Δt_m is called the **logarithmic mean temperature difference**. For the special case of $\Delta t_1 = \Delta t_2$ (possible only with a counterflow heat exchanger with equal capacities), which leads to an indeterminate form of Equation (15), $\Delta t_m = \Delta t_1 = \Delta t_2$.

Equation (15) for Δt_m is true only if the overall coefficient and the specific heat of the fluids are constant through the heat exchanger, and no heat losses occur (often well-approximated in practice). Parker et al. (1969) give a procedure for cases with variable overall coefficient U.

Calculations using Equation (14) and Δt_m are convenient when terminal temperatures are known. In many cases, however, the temperatures of the fluids leaving the exchanger are not known. To avoid trial-and-error calculations, an alternate method involves the use of three nondimensional parameters, defined as follows:

1. Exchanger Heat Transfer Effectiveness ε

$$\varepsilon = \frac{(t_{hi} - t_{ho})}{(t_{hi} - t_{ci})} \quad \text{when } C_h = C_{min}$$
$$\varepsilon = \frac{(t_{co} - t_{ci})}{(t_{hi} - t_{ci})} \quad \text{when } C_c = C_{min} \tag{16}$$

where

$C_h = (\dot{m}\, c_p)_h$ = hot fluid capacity rate, Btu/h·°F
$C_c = (\dot{m}\, c_p)_c$ = cold fluid capacity rate, Btu/h·°F
C_{min} = smaller of capacity rates C_h and C_c
t_h = terminal temperature of hot fluid, °F. Subscript *i* indicates entering condition; subscript *o* indicates leaving condition.
t_c = terminal temperature of cold fluid, °F. Subscripts *i* and *o* are the same as for t_h.

2. Number of Exchanger Heat Transfer Units (NTU)

$$\text{NTU} = \frac{AU_{avg}}{C_{min}} = \frac{1}{C_{min}} \int_A U\, dA \tag{17}$$

where A is the area used to define overall coefficient U.

3. Capacity Rate Ratio Z

$$Z = \frac{C_{min}}{C_{max}} \tag{18}$$

For a given exchanger, the heat transfer effectiveness can generally be expressed for a given exchanger as a function of the number of transfer units and the capacity rate ratio:

$$\varepsilon = f\,(\text{NTU, Z, flow arrangement}) \tag{19}$$

The effectiveness is independent of the temperatures in the exchanger. For any exchanger in which the capacity rate ratio Z is zero (where one fluid undergoes a phase change; e.g., in a condenser or evaporator), the effectiveness is

$$\varepsilon = 1 - \exp(-\text{NTU}) \tag{20}$$

Heat transferred can be determined from

$$q = C_h(t_{hi} - t_{ho}) = C_c(t_{co} - t_{ci}) \tag{21}$$

Combining Equations (16) and (21) produces an expression for heat transfer rate in terms of entering fluid temperatures:

$$q = \varepsilon C_{min}(t_{hi} - t_{ci}) \tag{22}$$

The proper mean temperature difference for Equation (14) is then given by

$$\Delta t_m = \frac{(t_{hi} - t_{ci})\varepsilon}{\text{NTU}} \tag{23}$$

The effectiveness for **parallel flow exchangers** is

$$\varepsilon = \frac{1 - \exp[-\text{NTU}\,(1 + Z)]}{1 + Z} \tag{24}$$

For $Z = 1$,

$$\varepsilon = \frac{1 - \exp(-2\ \text{NTU})}{2} \tag{25}$$

The effectiveness for **counterflow exchangers** is

$$\varepsilon = \frac{1 - \exp[-\text{NTU}(1 - Z)]}{1 - Z\exp[-\text{NTU}(1 - Z)]} \tag{26}$$

$$\varepsilon = \frac{\text{NTU}}{1 + \text{NTU}} \quad \text{for } Z = 1 \tag{27}$$

Incropera and DeWitt (1996) and Kays and London (1984) show the relations of ε, NTU, and Z for other flow arrangements. These authors and Afgan and Schlunder (1974) present graphical representations for convenience.

TRANSIENT HEAT FLOW

Often, the heat transfer and temperature distribution under unsteady-state (varying with time) conditions must be known. Examples are (1) cold storage temperature variations on starting or stopping a refrigeration unit; (2) variation of external air temperature and solar irradiation affecting the heat load of a cold storage room or wall temperatures; (3) the time required to freeze a given material under certain conditions in a storage room; (4) quick freezing of objects by direct immersion in brines; and (5) sudden heating or cooling of fluids and solids from one temperature to a different temperature.

The equations describing transient temperature distribution and heat transfer are presented in this section. Numerical methods are the simplest means of solving these equations because numerical data are easy to obtain. However, with some numerical solutions and off-the-shelf software, the physics that drives the energy transport can be lost. Thus, analytical solution techniques are also included in this section.

The fundamental equation for unsteady-state conduction in solids or fluids in which there is no substantial motion is

$$\frac{\partial t}{\partial \tau} = \alpha\left(\frac{\partial^2 t}{\partial x^2} + \frac{\partial^2 t}{\partial y^2} + \frac{\partial^2 t}{\partial z^2}\right) \tag{28}$$

where thermal diffusivity α is the ratio $k/\rho c_p$; k is thermal conductivity; ρ, density; and c_p, specific heat. If α is large (high conductivity, low density and specific heat, or both), heat will diffuse faster.

One of the most elementary transient heat transfer models predicts the rate of temperature change of a body or material being held at constant volume with uniform temperature, such as a well-stirred reservoir of fluid whose temperature is changing because of a net rate of heat gain or loss:

$$q_{net} = (Mc_p)\frac{dt}{d\tau} \tag{29}$$

where M is the mass of the body, c_p is the specific heat at constant pressure, and q_{net} is the net heat transfer rate to the substance (heat transfer into the substance is positive, and heat transfer out of the substance is negative). Equation (29) is applicable when the pressure around the substance is constant; if the volume of the substance is constant, c_p should be replaced by the constant volume specific heat c_v. It should be noted that with the density of solids and liquids being almost constant, the two specific heats are almost equal. The term q_{net} may include heat transfer by conduction, convection, or radiation and is the difference between the heat transfer rates into and out of the body.

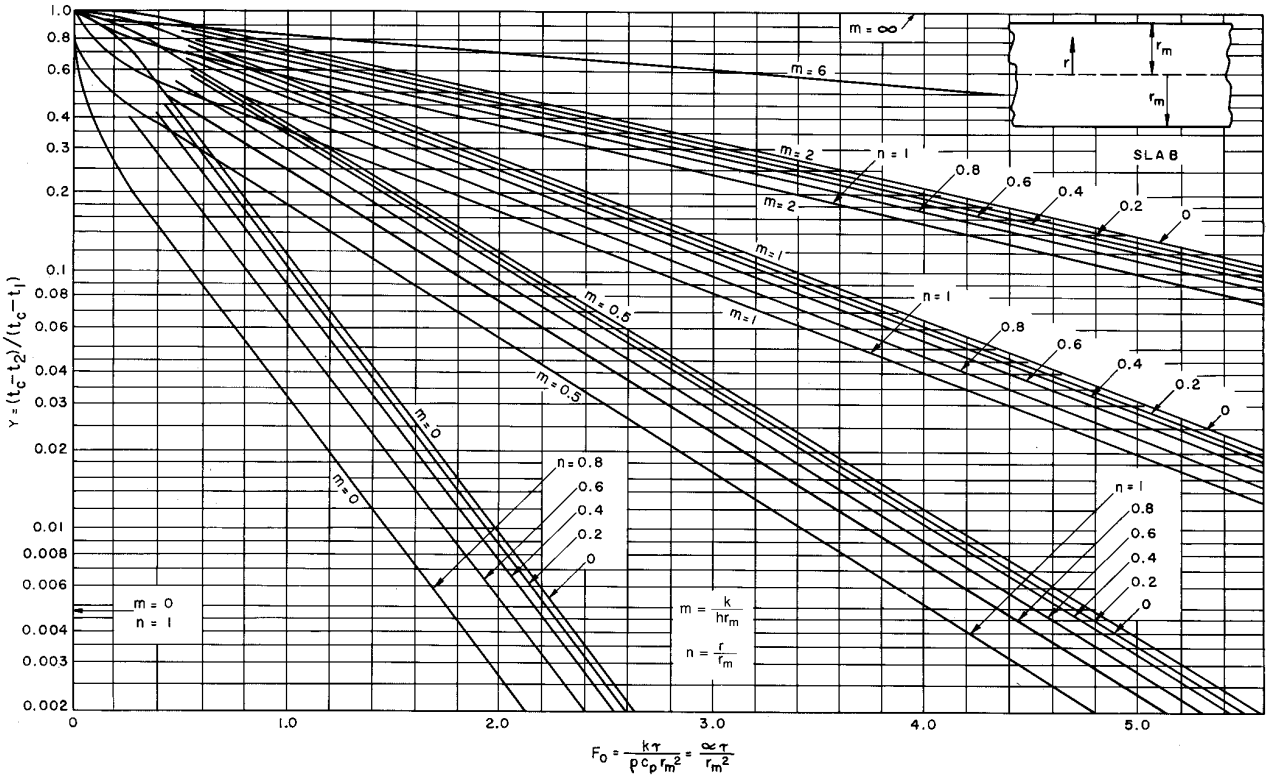

Fig. 2 Transient Temperatures for Infinite Slab

From Equations (28) and (29), it is possible to derive expressions for temperature and heat flow variations at different instants and different locations. Most common cases have been solved and presented in graphical forms (Jakob 1957, Schneider 1964, Myers 1971). In other cases, it is simpler to use numerical methods (Croft and Lilley 1977, Patankar 1980). When convective boundary conditions are required in the solution of Equations (28) and (29), h values based on steady-state correlations are often used. However, this approach may not be valid when rapid transients are involved.

Estimating Cooling Times

Cooling times for materials can be estimated (McAdams 1954) by Gurnie-Lurie charts (Figures 2, 3, and 4), which are graphical solutions for the heating or cooling of infinite slabs, infinite cylinders, and spheres. These charts assume an initial uniform temperature distribution and no change of phase. They apply to a body exposed to a constant temperature fluid with a constant surface convection coefficient of h.

Using Figures 2, 3, and 4, it is possible to estimate both the temperature at any point and the average temperature in a homogeneous mass of material as a function of time in a cooling process. It is possible to estimate cooling times for rectangular-shaped solids, cubes, cylinders, and spheres.

From the point of view of heat transfer, a cylinder insulated on its ends behaves like a cylinder of infinite length, and a rectangular solid insulated so that only two parallel faces allow heat transfer behaves like an infinite slab. A thin slab or a long, thin cylinder may be also considered infinite objects.

Consider a slab having insulated edges being cooled. If the cooling time is the time required for the center of the slab to reach a temperature of t_2, the cooling time can be calculated as follows:

1. Evaluate the temperature ratio $(t_c - t_2)/(t_c - t_1)$.

   where

   t_c = temperature of cooling medium
   t_1 = initial temperature of product
   t_2 = final temperature of product at center

   Note that in Figures 2, 3, and 4, the temperature ratio $(t_c - t_2)/(t_c - t_1)$ is designated as Y to simplify the equations.

2. Determine the radius ratio r/r_m designated as n in Figures 2, 3, and 4.

   where

   r = distance from centerline
   r_m = half thickness of slab

3. Evaluate the resistance ratio k/hr_m designated as m in Figures 2, 3, and 4.

   where

   k = thermal conductivity of material
   h = heat transfer coefficient

4. From Figure 2 for infinite slabs, select the appropriate value of $k\tau/\rho c_p r_m^2$ designated as F_o in Figures 2, 3, and 4.

   where

   τ = time elapsed
   c_p = specific heat
   ρ = density

5. Determine τ from the value of $k\tau/\rho c_p r_m^2$.

Multidimensional Temperature Distribution

The solution for semi-infinite slabs and cylinders (shown in Figures 2, 3, and 4) can be used to find the temperatures in finite rectangular solids or cylinders.

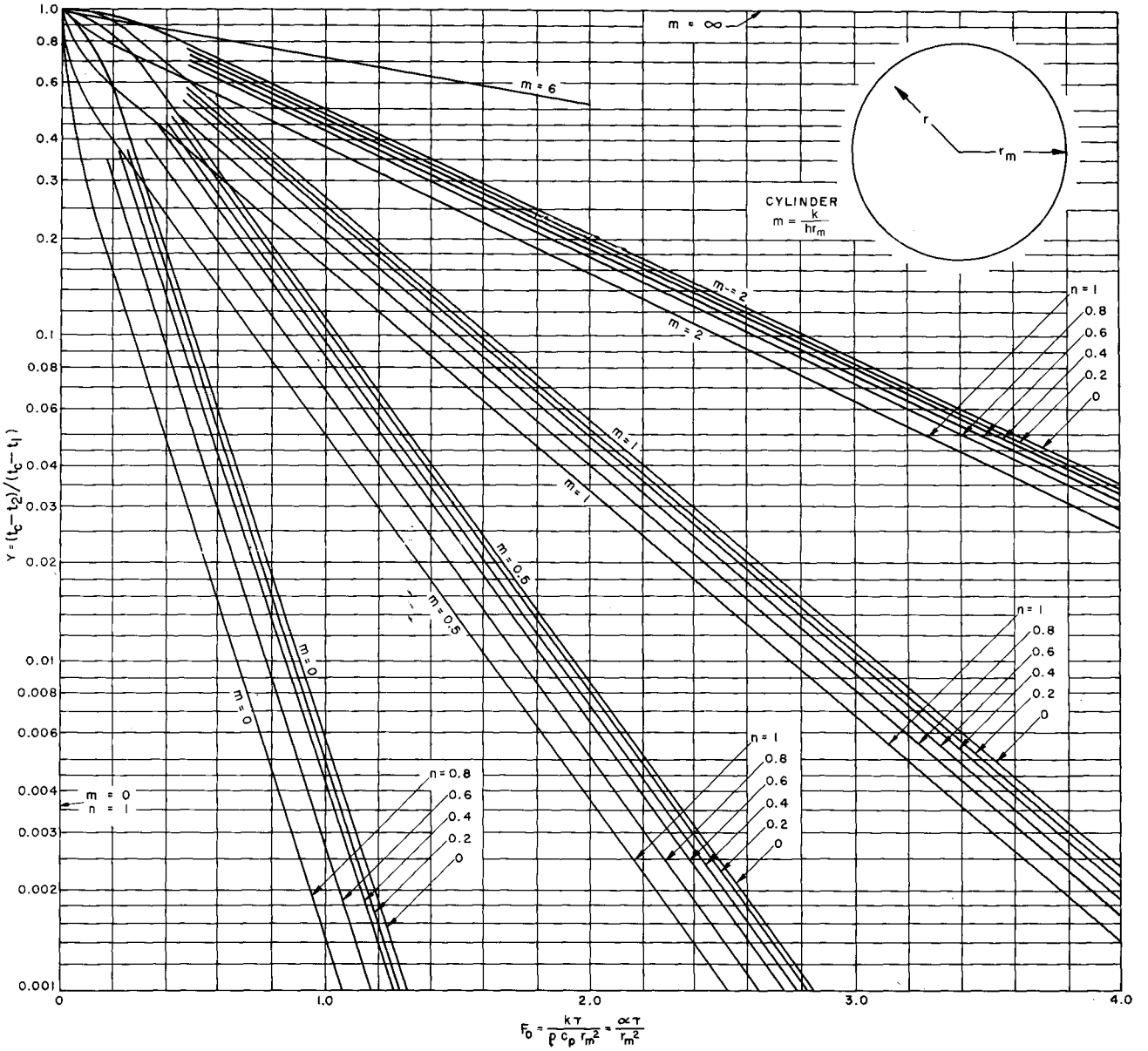

Fig. 3 Transient Temperatures for Infinite Cylinder

The temperature in the finite object can be calculated from the temperature ratio Y of the infinite objects that intersect to form the finite object. The product of the temperature ratios of the infinite objects is the temperature ratio of the finite object; for example, for the finite cylinder of Figure 5,

$$Y_{fc} = Y_{is} Y_{ic} \tag{30}$$

where

Y_{fc} = temperature ratio of finite cylinder
Y_{is} = temperature ratio of infinite slab
Y_{ic} = temperature ratio of infinite cylinder

For a finite rectangular solid,

$$Y_{frs} = (Y_{is})_1 (Y_{is})_2 (Y_{is})_3 \tag{31}$$

where Y_{frs} = temperature ratio of finite rectangular solid, and subscripts 1, 2, and 3 designate three infinite slabs. The convective heat transfer coefficients associated with one pair of parallel surfaces need not be equal to the coefficient associated with another pair. However, the temperature of the fluid adjacent to every surface should be the same. In evaluating the resistance ratio and the Fourier number Fo, the appropriate values of the heat transfer coefficient and the characteristic dimension should be used.

Heat Exchanger Transients

Determination of the transient behavior of heat exchangers is becoming increasingly important in evaluating the dynamic behavior of heating and air-conditioning systems. Many studies of the transient behavior of counterflow and parallel flow heat exchangers have been conducted; some are listed in the section on Bibliography.

THERMAL RADIATION

Radiation, one of the basic mechanisms for energy transfer between different temperature regions, is distinguished from conduction and convection in that it does not depend on an intermediate

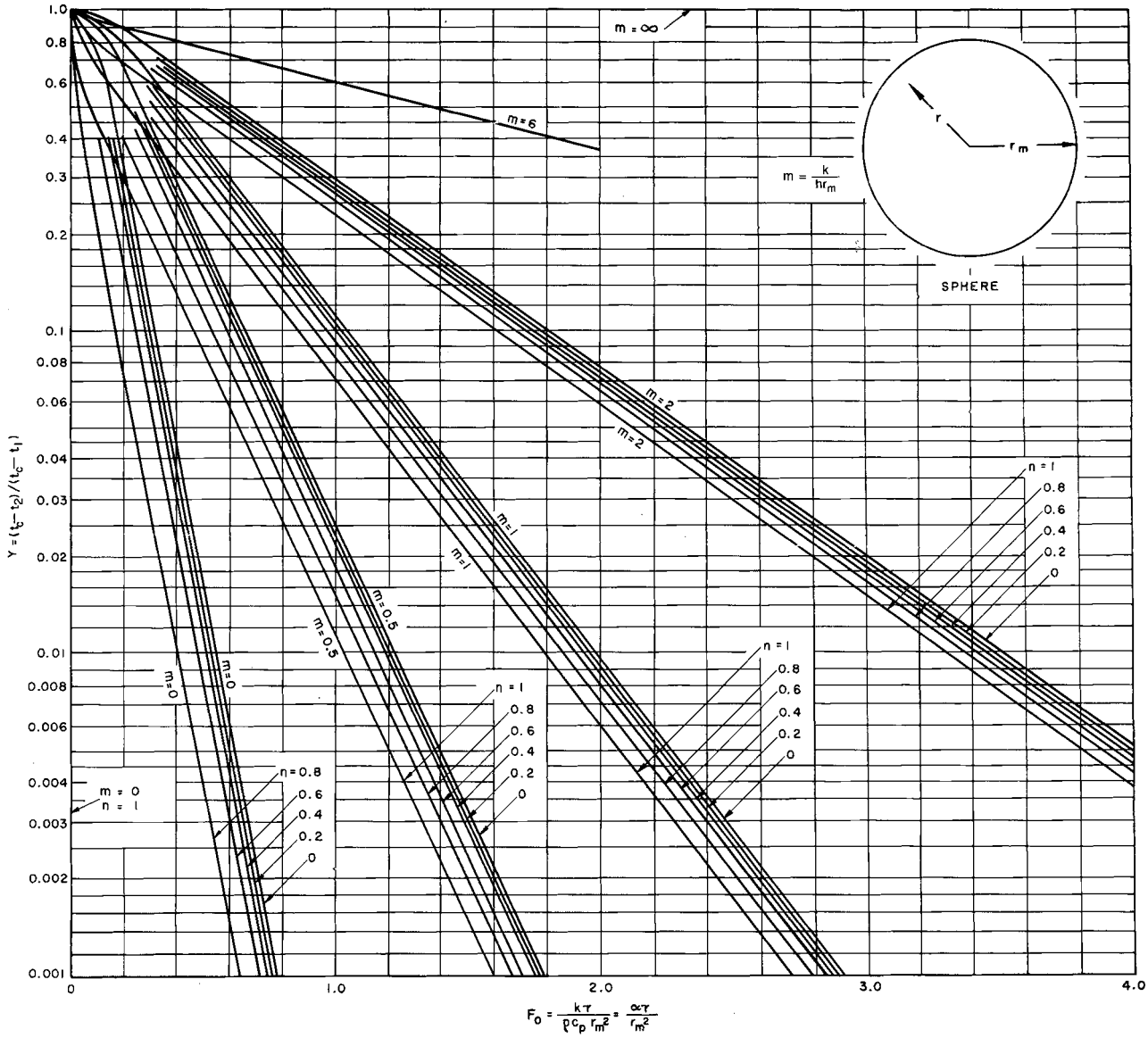

Fig. 4 Transient Temperatures for Spheres

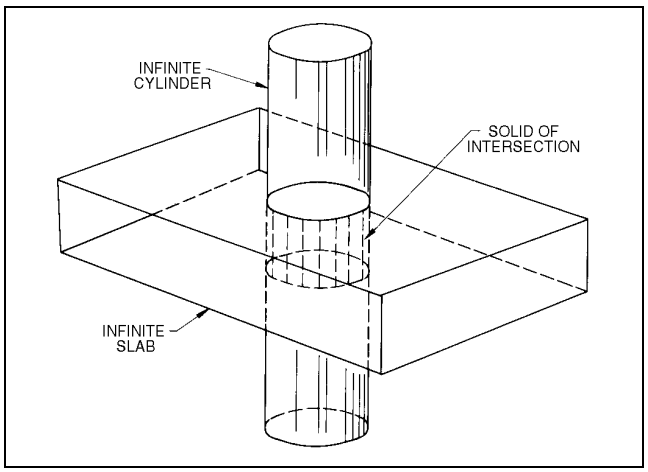

Fig. 5 Finite Cylinder of Intersection from Intersection of Infinite Cylinder and Infinite Slab

material as a carrier of energy but rather is impeded by the presence of material between the regions. The radiation energy transfer process is the consequence of energy-carrying electromagnetic waves that are emitted by atoms and molecules due to changes in their energy content. The amount and characteristics of radiant energy emitted by a quantity of material depend on the nature of the material, its microscopic arrangement, and its absolute temperature. Although rate of energy emission is independent of the surroundings, the **net** energy transfer rate depends on the temperatures and spatial relationships of the surface and its surroundings.

Blackbody Radiation

The rate of thermal radiant energy emitted by a surface depends on its absolute temperature. A surface is called **black** if it can absorb all incident radiation. The total energy emitted per unit time per unit area of black surface W_b to the hemispherical region above it is given by the **Stefan-Boltzmann law**.

$$W_b = \sigma T^4 \tag{32}$$

Table 3 Emittances and Absorptances for Some Surfaces[a]

Class	Surfaces	Total Normal Emittance[b]		Absorptance for Solar Radiation
		At 50 to 100 °F	At 1000 °F	
1	A small hole in a large box, sphere, furnace, or enclosure	0.97 to 0.99	0.97 to 0.99	0.97 to 0.99
2	Black nonmetallic surfaces such as asphalt, carbon, slate, paint, paper	0.90 to 0.98	0.90 to 0.98	0.85 to 0.98
3	Red brick and tile, concrete and stone, rusty steel and iron, dark paints (red, brown, green, etc.)	0.85 to 0.95	0.75 to 0.90	0.65 to 0.80
4	Yellow and buff brick and stone, firebrick, fireclay	0.85 to 0.95	0.70 to 0.85	0.50 to 0.70
5	White or light cream brick, tile, paint or paper, plaster, whitewash	0.85 to 0.95	0.60 to 0.75	0.30 to 0.50
6	Window glass	0.90	—	c
7	Bright aluminum paint; gilt or bronze paint	0.40 to 0.60	—	0.30 to 0.50
8	Dull brass, copper, or aluminum; galvanized steel; polished iron	0.20 to 0.30	0.30 to 0.50	0.40 to 0.65
9	Polished brass, copper, monel metal	0.02 to 0.05	0.05 to 0.15	0.30 to 0.50
10	Highly polished aluminum, tin plate, nickel, chromium	0.02 to 0.04	0.05 to 0.10	0.10 to 0.40
11	Selective surfaces			
	Stainless steel wire mesh	0.23 to 0.28	—	0.63 to 0.86
	White painted surface	0.92	—	0.23 to 0.49
	Copper treated with solution of $NaClO_2$ and NaOH	0.13	—	0.87
	Copper, nickel, and aluminum plate with CuO coating	0.09 to 0.21	—	0.08 to 0.93

[a]See also Chapter 36, McAdams (1954), and Siegel and Howell (1981).

[b]Hemispherical and normal emittance are unequal in many cases. The hemispherical emittance may vary from up to 30% greater for polished reflectors to 7% lower for nonconductors.

[c]Absorbs 4 to 40% depending on its transmittance.

where W_b is the total rate of energy emission per unit area, and σ is the Stefan-Boltzmann constant (0.1712×10^{-8} Btu/h·ft²·°R⁴).

The heat radiated by a body comprises electromagnetic waves of many different frequencies or wavelengths. Planck showed that the spectral distribution of the energy radiated by a blackbody is

$$W_{b\lambda} = \frac{C_1 \lambda^{-5}}{e^{C_2/\lambda T} - 1} \tag{33}$$

where

$W_{b\lambda}$ = monochromatic emissive power of blackbody, Btu/h·ft²·μm
λ = wavelength, μm
T = temperature, °R
C_1 = first Planck's law constant = 1.1870×10^8 Btu·μm⁴/h·ft²
C_2 = second Planck's law constant = 2.5896×10^4 μm·°R

$W_{b\lambda}$ is the **monochromatic emissive power**, defined as the energy emitted per unit time per unit surface area at wavelength λ per unit wavelength interval around λ; that is, the energy emitted per unit time per unit surface area in the interval $d\lambda$ is equal to $W_{b\lambda}d\lambda$.

The Stefan-Boltzmann equation can be obtained by integrating Planck's equation:

$$W_b = \sigma T^4 = \int_0^\infty W_{b\lambda} d\lambda \tag{34}$$

Wien showed that the wavelength of maximum emissive power multiplied by the absolute temperature is a constant:

$$\lambda_{max} T = 5216 \ \mu m \cdot {}^\circ R \tag{35}$$

where λ_{max} is the wavelength at which the monochromatic emissive power is a maximum and not the maximum wavelength. Equation (35) is known as **Wien's displacement law**. According to this law, the maximum spectral emissive power is displaced to shorter wavelengths with increasing temperature, such that significant emission eventually occurs over the entire visible spectrum as shorter wavelengths become more prominent. For additional details, see Incropera and DeWitt (1996).

Actual Radiation

Substances and surfaces diverge variously from the Stefan-Boltzmann and Planck laws. W_b and $W_{b\lambda}$ are the maximum emissive powers at a surface temperature. Actual surfaces emit and absorb less than these maximums and are called **nonblack**. The emissive power of a nonblack surface at temperature T radiating to the hemispherical region above it is written as

$$W = \varepsilon W_b = \varepsilon \sigma T^4 \tag{36}$$

where ε is known as the **hemispherical emittance**. The term emittance conforms to physical and electrical terminology; the suffix "ance" denotes a property of a piece of material as it exists. The ending "ivity" denotes a property of the bulk material independent of geometry or surface condition. Thus, emittance, reflectance, absorptance, and transmittance refer to actual pieces of material. Emissivity, reflectivity, absorptivity, and transmissivity refer to the properties of materials that are optically smooth and thick enough to be opaque.

The emittance is a function of the material, the condition of its surface, and the temperature of the surface. Table 3 lists selected values; Siegel and Howell (1981) and Modest (1993) have more extensive lists.

The monochromatic emissive power of a nonblack surface is similarly written as

$$W_\lambda = \varepsilon_\lambda W_{b\lambda} = \varepsilon_\lambda \left(\frac{C_1 \lambda^{-5}}{e^{C_2/\lambda T} - 1} \right) \tag{37}$$

where ε_λ is the monochromatic hemispherical emittance. The relationship between ε and ε_λ is given by

$$W = \varepsilon \sigma T^4 = \int_0^\infty W_\lambda d\lambda = \int_0^\infty \varepsilon_\lambda W_{b\lambda} d\lambda$$

or

$$\varepsilon = \frac{1}{\sigma T^4} \int_0^\infty \varepsilon_\lambda W_{b\lambda} d\lambda \tag{38}$$

If ε_λ does not depend on λ, then, from Equation (38), $\varepsilon = \varepsilon_\lambda$. Surfaces with this characteristic are called **gray**. Gray surface characteristics are often assumed in calculations. Several classes of surfaces approximate this condition in some regions of the spectrum. The simplicity is desirable, but care must be exercised, especially if

temperatures are high. Assumption of grayness is sometimes made because of the absence of information relating ε_λ and λ.

When radiant energy falls on a surface, it can be absorbed, reflected, or transmitted through the material. Therefore, from the first law of thermodynamics,

$$\alpha + \tau + \rho = 1 \tag{39}$$

where

α = fraction of incident radiation absorbed or **absorptance**
τ = fraction of incident radiation transmitted or **transmittance**
ρ = fraction of incident radiation reflected or **reflectance**

If the material is opaque, as most solids are in the infrared, $\tau = 0$ and $\alpha + \rho = 1$. For a black surface, $\alpha = 1$, $\rho = 0$, and $\tau = 0$. Platinum black and gold black are as black as any actual surface and have absorptances of about 98% in the infrared. Any desired degree of blackness can be simulated by a small hole in a large enclosure. Consider a ray of radiant energy entering the opening. It will undergo many internal reflections and be almost completely absorbed before it has a reasonable probability of passing back out of the opening.

Certain flat black paints also exhibit emittances of 98% over a wide range of conditions. They provide a much more durable surface than gold or platinum black and are frequently used on radiation instruments and as standard reference in emittance or reflectance measurements.

Kirchhoff's law relates emittance and absorptance of any opaque surface from thermodynamic considerations; it states that for any surface where the incident radiation is independent of angle or where the surface is diffuse, $\varepsilon_\lambda = \alpha_\lambda$. If the surface is gray, or the incident radiation is from a black surface at the same temperature, then $\varepsilon = \alpha$ as well, but many surfaces are not gray. For most surfaces listed in Table 3, absorptance for solar radiation is different from emittance for low-temperature radiation. This is because the wavelength distributions are different in the two cases, and ε_λ varies with wavelength.

The foregoing discussion relates to total hemispherical radiation from surfaces. Energy distribution over the hemispherical region above the surface also has an important effect on the rate of heat transfer in various geometric arrangements.

Lambert's law states that the emissive power of radiant energy over a hemispherical surface above the emitting surface varies as the cosine of the angle between the normal to the radiating surface and the line joining the radiating surface to the point of the hemispherical surface. This radiation is **diffuse radiation**. The Lambert emissive power variation is equivalent to assuming that radiation from a surface in a direction other than normal occurs as if it came from an equivalent area with the same emissive power (per unit area) as the original surface. The equivalent area is obtained by projecting the original area onto a plane normal to the direction of radiation. Black surfaces obey the Lambert law exactly. The law is approximate for many actual radiation and reflection processes, especially those involving rough surfaces and nonmetallic materials. Most radiation analyses are based on the assumption of gray diffuse radiation and reflection.

In estimating heat transfer rates between surfaces of different geometries, radiation characteristics, and orientations, it is usually assumed that

- All surfaces are gray or black
- Radiation and reflection are diffuse
- Properties are uniform over the surfaces
- Absorptance equals emittance and is independent of the temperature of the source of incident radiation
- The material in the space between the radiating surfaces neither emits nor absorbs radiation

These assumptions greatly simplify problems, although results must be considered approximate.

Angle Factor

The distribution of radiation from a surface among the surfaces it irradiates is indicated by a quantity variously called an interception, a view, a configuration, a shape factor, or an angle factor. In terms of two surfaces i and j, the **angle factor** F_{ij} from surface i to surface j is the ratio of the radiant energy leaving surface i and directly reaching surface j to the total radiant energy leaving surface i. The angle factor from j to i is similarly defined, merely by interchanging the roles of i and j. This second angle factor is not, in general, numerically equal to the first. However, the reciprocity relation $F_{ij}A_i = F_{ji}A_j$, where A is the surface area, is always valid. Note that a concave surface may "see itself" ($F_{ii} \neq 0$), and that if n surfaces form an enclosure,

$$\sum_{j=1}^{n} F_{ij} = 1 \tag{40}$$

The angle factor F_{12} between two surfaces is

$$F_{12} = \frac{1}{A_1}\int_{A_1}\int_{A_2} \frac{\cos\phi_1 \cos\phi_2}{\pi r^2}\, dA_1\, dA_2 \tag{41}$$

where dA_1, and dA_2 are elemental areas of the two surfaces, r is the distance between dA_1 and dA_2, and ϕ_1 and ϕ_2 are the angles between the respective normals to dA_1 and dA_2 and the connecting line r. Numerical, graphical, and mechanical techniques can solve this equation (Siegel and Howell 1981, Modest 1993). Numerical values of the angle factor for common geometries are given in Figure 6.

Calculation of Radiant Exchange Between Surfaces Separated by Nonabsorbing Media

A surface radiates energy at a rate independent of its surroundings and absorbs and reflects incident energy at a rate dependent on its surface condition. The net energy exchange per unit area is denoted by q or q_j for unit area A_j. It is the rate of emission of the surface minus the total rate of absorption at the surface from all radiant effects in its surroundings, possibly including the return of some of its own emission by reflection off its surroundings. The rate at which energy must be supplied to the surface by other exchange processes if its temperature is to remain constant is q; therefore, to define q, the total radiant surroundings (in effect, an enclosure) must be specified.

Several methods have been developed to solve certain problems. To calculate the radiation exchange at each surface of an enclosure of n opaque surfaces by simple, general equations convenient for machine calculation, two terms must be defined:

G = irradiation; total radiation incident on surface per unit time and per unit area
J = radiosity; total radiation that leaves surface per unit time and per unit area

The radiosity is the sum of the energy emitted and the energy reflected:

$$J = \varepsilon W_b + \rho G \tag{42}$$

Because the transmittance is zero, the reflectance is

$$\rho = 1 - \alpha = 1 - \varepsilon$$

Thus,

$$J = \varepsilon W_b + (1 - \varepsilon)G \tag{43}$$

The net energy lost by a surface is the difference between the radiosity and the irradiation:

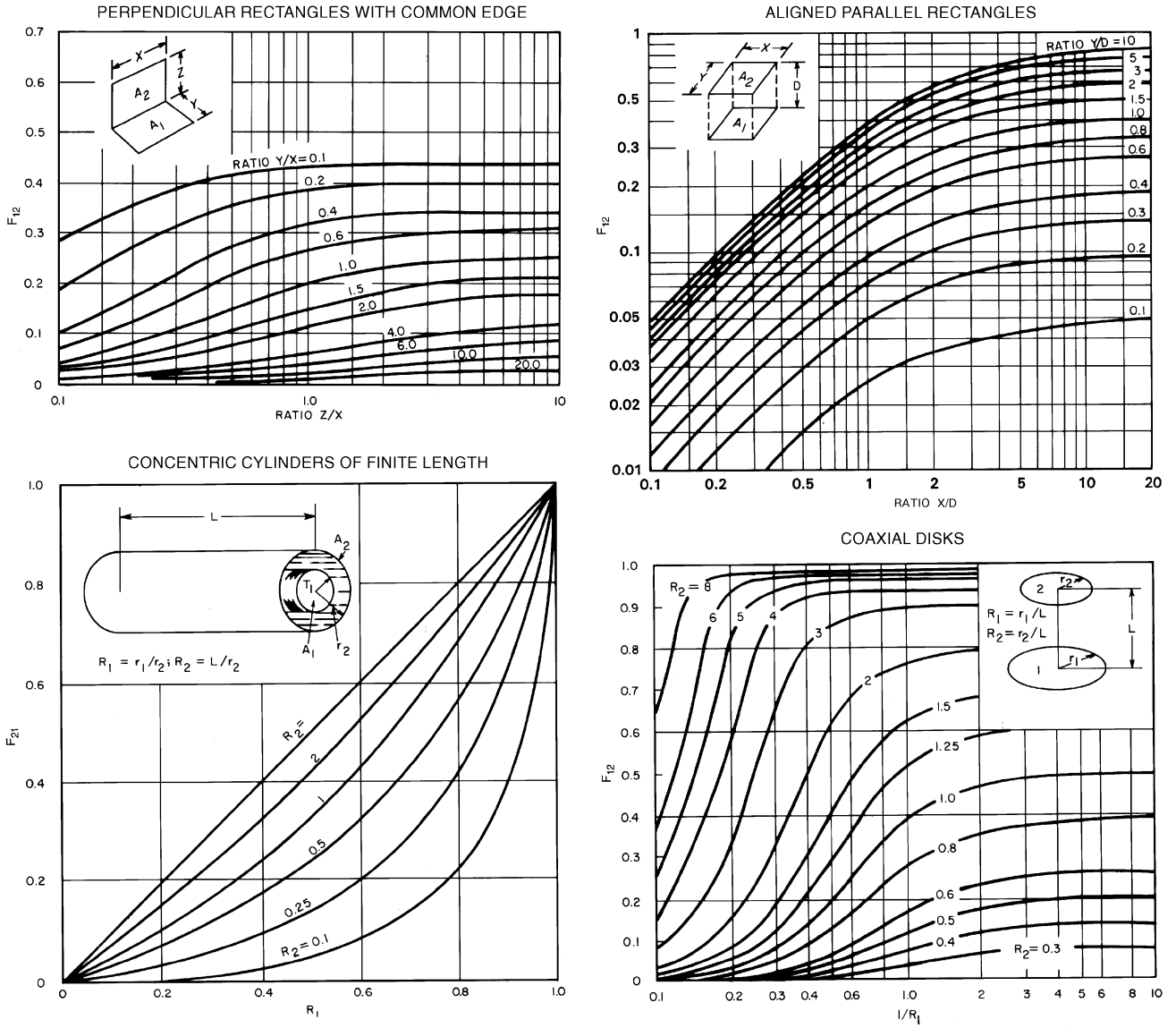

Fig. 6 Radiation Angle Factor for Various Geometries

$$q/A = J - G = \varepsilon W_b + (1-\varepsilon)G - G \tag{44}$$

Substituting for G in terms of J from Equation (43),

$$q = \frac{W_b - J}{(1-\varepsilon)/\varepsilon A} \tag{45}$$

Consider an enclosure of n isothermal surfaces with areas of $A_1, A_2, \ldots, A_n$, emittances of $\varepsilon_1, \varepsilon_2, \ldots, \varepsilon_n$, and reflectances of $\rho_1, \rho_2, \ldots, \rho_n$, respectively.

The irradiation of surface i is the sum of the radiation incident on it from all n surfaces:

$$G_i A_i = \sum_{j=1}^{n} F_{ji} J_j A_j = \sum_{j=1}^{n} F_{ij} J_j A_i$$

or

$$G_i = \sum_{j=1}^{n} F_{ij} J_j$$

Substituting in Equation (44) yields the following simultaneous equations when each of the n surfaces is considered:

$$J_i = \varepsilon_i W_{bi} + (1-\varepsilon_i) \sum_{j=1}^{n} F_{ij} J_j \qquad i = 1, 2, \ldots, n \tag{46}$$

Equation (46) can be solved manually for the unknown Js if the number of surfaces is small. The solution for more complex enclosures requires a computer.

Once the radiosities (Js) are known, the net radiant energy lost by each surface is determined from Equation (45) as

$$q_i = \frac{W_{bi} - J_i}{(1-\varepsilon_i)/\varepsilon_i A_i}$$

If the surface is black, Equation (45) becomes indeterminate, and an alternate expression must be used, such as

$$q_i = \sum_{j=1}^{n} J_i A_i F_{ij} - J_j A_j F_{ji}$$

or

$$q_i = \sum_{j=1}^{n} F_{ij} A_i (J_i - J_j) \quad (47)$$

since

$$F_{ij} A_i = F_{ji} A_j$$

All diffuse radiation processes are included in the aforementioned enclosure method, and surfaces with special characteristics are assigned consistent properties. An opening is treated as an equivalent surface area A_e with a reflectance of zero. If energy enters the enclosure diffusely through the opening, A_e is assigned an equivalent temperature; otherwise, its temperature is taken as zero. If the loss through the opening is desired, q_2 is found. A window in the enclosure is assigned its actual properties.

A surface in **radiant balance** is one for which radiant emission is balanced by radiant absorption; heat is neither removed from nor supplied to the surface. Reradiating surfaces (insulated surfaces with $q_{net} = 0$), can be treated in Equation (46) as being perfectly reflective (i.e., $\varepsilon = 0$). The equilibrium temperature of such a surface can be found from

$$T_k = \left(\frac{J_k}{\sigma}\right)^{0.25}$$

once Equation (46) has been solved for the radiosities.

Use of angle factors and radiation properties as defined assumes that the surfaces are diffuse radiators—a good assumption for most nonmetals in the infrared region, but a poor assumption for highly polished metals. Subdividing the surfaces and considering the variation of radiation properties with angle of incidence improves the approximation but increases the work required for a solution.

Radiation in Gases

Elementary gases such as oxygen, nitrogen, hydrogen, and helium are essentially transparent to thermal radiation. Their absorption and emission bands are confined mainly to the ultraviolet region of the spectrum. The gaseous vapors of most compounds, however, have absorption bands in the infrared region. Carbon monoxide, carbon dioxide, water vapor, sulfur dioxide, ammonia, acid vapors, and organic vapors absorb and emit significant amounts of energy.

Radiation exchange by opaque solids is considered a surface phenomenon. Radiant energy does, however, penetrate the surface of all materials. The absorption coefficient gives the rate of exponential attenuation of the energy. Metals have large absorption coefficients, and radiant energy penetrates only a few hundred angstroms at most. Absorption coefficients for nonmetals are lower. Radiation may be considered a surface phenomenon unless the material is transparent. Gases have small absorption coefficients, so the path length of radiation through gas becomes very significant.

Beer's law states that the attenuation of radiant energy in a gas is a function of the product $p_g L$ of the partial pressure of the gas and the path length. The monochromatic absorptance of a body of gas of thickness L is then given by

$$\alpha_{\lambda L} = 1 - e^{-\alpha \lambda L} \quad (48)$$

Because absorption occurs in discrete wavelengths, the absorptances must be summed over the spectral region corresponding to the temperature of the blackbody radiation passing through the gas.

Table 4 Emittance of CO_2 and Water Vapor in Air at 75 °F

Path Length, ft	CO_2, % by Volume		Relative Humidity, %			
	0.1	0.3	1.0	10	50	100
10	0.03	0.06	0.09	0.06	0.17	0.22
100	0.09	0.12	0.16	0.22	0.39	0.47
1000	0.16	0.19	0.23	0.47	0.64	0.70

The monochromatic absorption coefficient α_λ is also a function of temperature and pressure of the gas; therefore, detailed treatment of gas radiation is quite complex.

Estimated emittance for carbon dioxide and water vapor in air at 75°F is a function of concentration and path length (Table 4). The values are for a hemispherically shaped body of gas radiating to an element of area at the center of the hemisphere. Among others, Modest (1993), Siegel and Howell (1981), and Hottel and Sarofim (1967) describe geometrical calculations in their texts on radiation transfer. Generally, at low values of $p_g L$, the mean path length L (or equivalent hemispherical radius for a gas body radiating to its surrounding surfaces) is four times the mean hydraulic radius of the enclosure. A room with a dimensional ratio of 1:1:4 has a mean path length of 0.89 times the shortest dimension when considering radiation to all walls. For a room with a dimensional ratio of 1:2:6, the mean path length for the gas radiating to all surfaces is 1.2 times the shortest dimension. The mean path length for radiation to the 2 by 6 face is 1.18 times the shortest dimension. These values are for cases where the partial pressure of the gas times the mean path length approaches zero ($p_g L \approx 0$). The factor decreases with increasing values of $p_g L$. For average rooms with approximately 8 ft ceilings and relative humidity ranging from 10 to 75% at 75°F, the effective path length for carbon dioxide radiation is about 85% of the ceiling height, or 6.8 ft. The effective path length for water vapor is about 93% of the ceiling height, or 7.4 ft. The effective emittance of the water vapor and carbon dioxide radiating to the walls, ceiling, and floor of a room 16 ft by 48 ft with 8 ft ceilings is in the following tabulation.

Relative Humidity, %	ε_g
10	0.10
50	0.19
75	0.22

The radiation heat transfer from the gas to the walls is then

$$q = \sigma A_w \varepsilon_g (T_g^4 - T_w^4) \quad (49)$$

The examples in Table 4 and the preceding text indicate the importance of gas radiation in environmental heat transfer problems. Gas radiation in large furnaces is the dominant mode of heat transfer, and many additional factors must be considered. Increased pressure broadens the spectral bands, and interaction of different radiating species prohibits simple summation of the emittance factors for the individual species. Departures from blackbody conditions necessitate separate calculations of the emittance and absorptance. McAdams (1954) and Hottel and Sarofim (1967) give more complete treatments of gas radiation.

NATURAL CONVECTION

Heat transfer involving motion in a fluid due to the difference in density and the action of gravity is called **natural convection** or **free convection**. Heat transfer coefficients associated with gases for natural convection are generally much lower than those for forced convection, and it is therefore important not to ignore radiation in calculating the total heat loss or gain. Radiant transfer may be of the same order of magnitude as natural convection, even at room

Table 5 Natural Convection Heat Transfer Coefficients

I. General relationships	$\mathrm{Nu} = c(\mathrm{Gr\,Pr})^n$	(1)
	$h = c\frac{k}{L}\left(\frac{L^3\rho^2\beta g\Delta t}{\mu^2}\right)_f^n\left(\frac{\mu c_p}{k}\right)_f^n$	(2)
Characteristic length L		
Vertical plates or pipes	L = height	
Horizontal plates	L = length	
Horizontal pipes	L = diameter	
Spheres	L = 0.5 × diameter	
Rectangular block, with horizontal length L_h and vertical length L_v	$1/L = (1/L_h) + (1/L_v)$	
II. Planes and pipes		
Horizontal or vertical planes, pipes, rectangular blocks, and spheres (excluding horizontal plates facing downward for heating and upward for cooling)		
(a) Laminar range, when Gr Pr is between 10^4 and 10^8	$\mathrm{Nu} = 0.56(\mathrm{Gr\,Pr})^{0.25}$	(3)
(b) Turbulent range, when Gr Pr is between 10^8 and 10^{12}	$\mathrm{Nu} = 0.13(\mathrm{Gr\,Pr})^{0.33}$	(4)
III. Wires		
For horizontal or vertical wires, use L = diameter, for Gr Pr between 10^{-7} and 1	$\mathrm{Nu} = (\mathrm{Gr\,Pr})^{0.1}$	(5)
IV. With air		
$\mathrm{Gr\,Pr} = 1.6 \times 10^6 L^3\Delta t$ (at 70°F, L in ft, Δt in °F)		
(a) Horizontal cylinders		
Small cylinder, laminar range	$h = 0.27(\Delta t/L)^{0.25}$	(6)
Large cylinder, turbulent range	$h = 0.18(\Delta t)^{0.33}$	(7)
(b) Vertical plates		
Small plates, laminar range	$h = 0.29(\Delta t/L)^{0.25}$	(8)
Large plates, turbulent range	$h = 0.19(\Delta t)^{0.33}$	(9)
(c) Horizontal plates, facing upward when heated or downward when cooled		
Small plates, laminar range	$h = 0.27(\Delta t/L)^{0.25}$	(10)
Large plates, turbulent range	$h = 0.22(\Delta t)^{0.33}$	(11)
(d) Horizontal plates, facing downward when heated or upward when cooled		
Small plates	$h = 0.12(\Delta t/L)^{0.25}$	(12)

temperatures, because wall temperatures in a room can affect human comfort (see Chapter 8).

Natural convection is important in a variety of heating and refrigeration equipment: (1) gravity coils used in high-humidity cold storage rooms and in roof-mounted refrigerant condensers, (2) the evaporator and condenser of household refrigerators, (3) baseboard radiators and convectors for space heating, and (4) cooling panels for air conditioning. Natural convection is also involved in heat loss or gain to equipment casings and interconnecting ducts and pipes.

Consider heat transfer by natural convection between a cold fluid and a hot surface. The fluid in immediate contact with the surface is heated by conduction, becomes lighter, and rises because of the difference in density of the adjacent fluid. The viscosity of the fluid resists this motion. The heat transfer is influenced by (1) gravitational force due to thermal expansion, (2) viscous drag, and (3) thermal diffusion. Gravitational acceleration g, coefficient of thermal expansion β, kinematic viscosity $v = \mu/\rho$, and thermal diffusivity $\alpha = k/\rho c_p$ affect natural convection. These variables are included in the dimensionless numbers given in Equation (1) in Table 5. The Nusselt number Nu is a function of the product of the Prandtl number Pr and the Grashof number Gr. These numbers, when combined, depend on the fluid properties, the temperature difference Δt between the surface and the fluid, and the characteristic length L of the surface. The constant c and the exponent n depend on the physical configuration and the nature of flow.

Natural convection cannot be represented by a single value of exponent n, but it can be divided into three regions:

1. **Turbulent** natural convection, for which n equals 0.33
2. **Laminar** natural convection, for which n equals 0.25
3. A region that has GrPr less than for laminar natural convection, for which the exponent n gradually diminishes from 0.25 to lower values

Note that for wires, the GrPr is likely to be very small, so that the exponent n is 0.1 [Equation (5) in Table 5].

To calculate the natural-convection heat transfer coefficient, determine GrPr to find whether the boundary layer is laminar or turbulent; then apply the appropriate equation from Table 5. The correct characteristic length indicated in the table must be used. Because the exponent n is 0.33 for a turbulent boundary layer, the characteristic length cancels out in Equation (2) in Table 5, and the heat transfer coefficient is independent of the characteristic length, as seen in Equations (7), (9), and (11) in Table 5. Turbulence occurs when length or temperature difference is large. Because the length of a pipe is generally greater than its diameter, the heat transfer coefficient for vertical pipes is larger than for horizontal pipes.

Convection from horizontal plates facing downward when heated (or upward when cooled) is a special case. Because the hot air is above the colder air, theoretically no convection should occur. Some convection is caused, however, by secondary influences such as temperature differences on the edges of the plate. As an approximation, a coefficient of somewhat less than half the coefficient for a heated horizontal plate facing upward can be used.

Because air is often the heat transport fluid, simplified equations for air are given in Table 5. Other information on natural convection is available in the section on Bibliography under Heat Transfer, General.

Observed differences in the comparison of recent experimental and numerical results with existing correlations for natural convective heat transfer coefficients indicate that caution should be used when applying coefficients for (isolated) vertical plates to vertical surfaces in enclosed spaces (buildings). Bauman et al. (1983) and

Altmayer et al. (1983) developed improved correlations for calculating natural convective heat transfer from vertical surfaces in rooms under certain temperature boundary conditions.

Natural convection can affect the heat transfer coefficient in the presence of weak forced convection. As the forced-convection effect (i.e., the Reynolds number) increases, "mixed convection" (superimposed forced-on-free convection) gives way to the pure forced-convection regime. In these cases, other sources describing combined free and forced convection should be consulted, since the heat transfer coefficient in the mixed-convection region is often larger than that calculated based on the natural- or forced-convection calculation alone. Metais and Eckert (1964) summarize natural-, mixed-, and forced-convection regimes for vertical and horizontal tubes. Figure 7 shows the approximate limits for horizontal tubes. Other studies are described by Grigull et al. (1982).

FORCED CONVECTION

Forced air coolers and heaters, forced air- or water-cooled condensers and evaporators, and liquid suction heat exchangers are examples of equipment that transfer heat primarily by forced convection.

When fluid flows over a flat plate, a **boundary layer** forms adjacent to the plate. The velocity of the fluid at the plate surface is zero and increases to its maximum free stream value just past the edge of the boundary layer (Figure 8). Boundary layer formation is important because the temperature change from plate to fluid (thermal resistance) is concentrated here. Where the boundary layer is thick, thermal resistance is great and the heat transfer coefficient is small. Flow within the boundary layer immediately downstream from the leading edge is laminar and is known as **laminar forced convection**. As flow proceeds along the plate, the laminar boundary layer increases in thickness to a critical value. Then, turbulent eddies develop within the boundary layer, except for a thin **laminar sublayer** adjacent to the plate.

The boundary layer beyond this point is a **turbulent boundary layer**, and the flow is **turbulent forced convection**. The region between the breakdown of the laminar boundary layer and the establishment of the turbulent boundary layer is the **transition region**. Because the turbulent eddies greatly enhance heat transport into the main stream, the heat transfer coefficient begins to increase rapidly through the transition region. For a flat plate with a smooth leading edge, the turbulent boundary layer starts at Reynolds numbers, based on distance from the leading edge, of about 300,000 to 500,000. In blunt-edged plates, it can start at much smaller Reynolds numbers.

For long tubes or channels of small hydraulic diameter, at sufficiently low flow velocity, the laminar boundary layers on each wall grow until they meet. Beyond this point, the velocity distribution does not change, and no transition to turbulent flow takes place. This is called **fully developed laminar flow**. For tubes of large diameter or at higher velocities, transition to turbulence takes place and **fully developed turbulent flow** is established (Figure 9). Therefore, the length dimension that determines the critical Reynolds number is the hydraulic diameter of the channel. For smooth circular tubes, flow is laminar for Reynolds numbers below 2100 and turbulent above 10,000.

Table 6 lists various forced-convection correlations. In the generalized, dimensionless formula of Equation (1) in Table 6, heat transfer is determined by flow conditions and by the fluid properties, as indicated by the Reynolds number and the Prandtl number. This equation can be modified to Equation (4) in Table 6 to get the **heat transfer factor** j. The heat transfer factor is related to the **friction factor** f by the interrelationship of the transport of momentum and heat; it is approximately $f/2$ for turbulent flow in straight ducts. These factors are plotted in Figure 10.

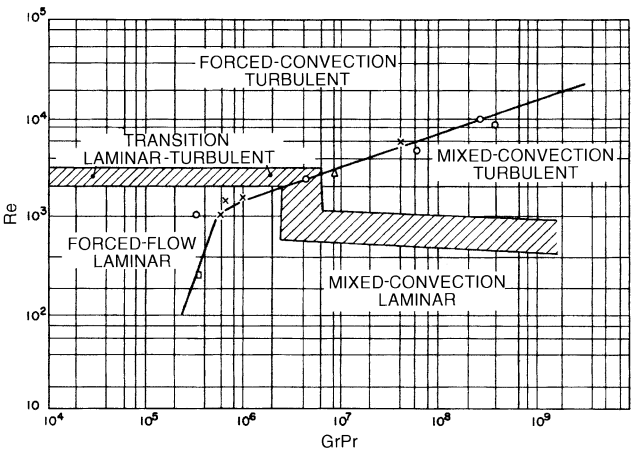

Fig. 7 Regimes of Free, Forced, and Mixed Convection for Flow-Through Horizontal Tubes

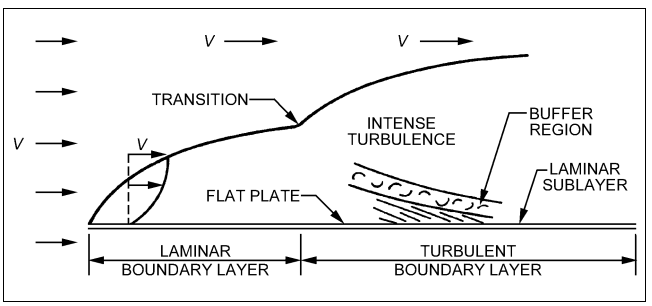

Fig. 8 Boundary Layer Buildup on Flat Plate (Vertical Scale Magnified)

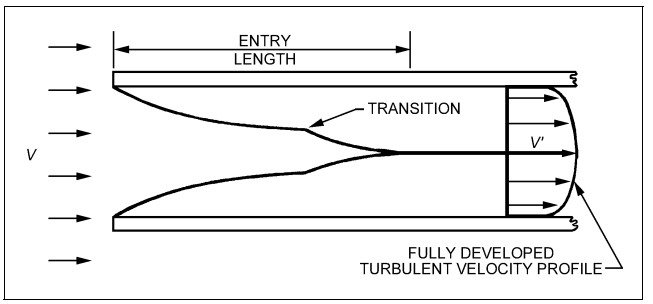

Fig. 9 Boundary Layer Buildup in Entry Length of Tube or Channel

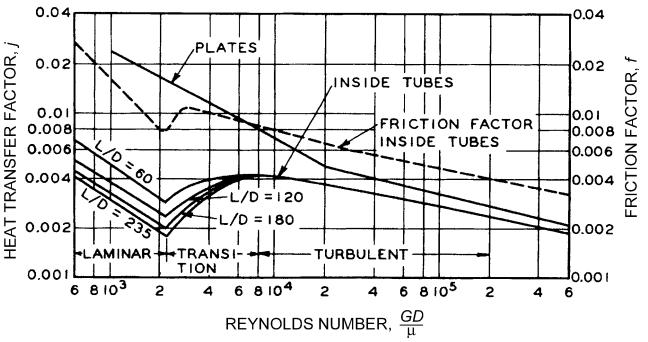

Fig. 10 Typical Dimensionless Representation of Forced-Convection Heat Transfer

Table 6 Equations for Forced Convection

Description	Reference: Author	Page	Eq. No.	Equation		
I. Generalized correlations						
(a) Turbulent flow inside tubes	Jakob	491	(23-36)	$\frac{hD}{k} = c\left(\frac{GD}{\mu}\right)^m\left(\frac{\mu c_p}{k}\right)^n$		(1)
(1) Using fluid properties based on bulk temperature t	McAdams	219	(9-10a)	$\frac{hD}{k} = 0.023\left(\frac{GD}{\mu}\right)^{0.8}\left(\frac{\mu c_p}{k}\right)^{0.4}$	(See Note a)	(2)
(2) Same as (1), except μ at surface temperature t_s	McAdams	219	(9-10c)	$\frac{h}{c_p G}\left(\frac{c_p\mu}{k}\right)^{2/3}\left(\frac{\mu_s}{\mu}\right)^{0.14} = \frac{0.023}{(GD/\mu)^{0.2}}$		(3)
(3) Using fluid properties based on film temperature $t_f = 0.5(t_s + t)$, except c_p in Stanton modulus	McAdams	219	(9-10b)	$\frac{h}{c_p G}\left(\frac{c_p\mu}{k}\right)_f^{2/3} = \frac{0.023}{(GD/\mu_f)^{0.2}} = j$		(4)
(4) For viscous fluids (viscosities higher than twice water), using viscosity μ at bulk temperature t and μ_s at surface temperature t_s	Jakob	547	(26-12)	$\frac{hD}{k} = 0.027\left(\frac{GD}{\mu}\right)^{0.8}\left(\frac{\mu c_p}{k}\right)^{1/3}\left(\frac{\mu}{\mu_s}\right)^{0.14}$		(5)
(b) Laminar flow inside tubes						
(1) For large D or high Δt, the effect of natural convection should be included	Jakob	544	(26-5)	$\frac{hD}{k} = 1.86\left[\left(\frac{GD}{\mu}\right)\left(\frac{c_p\mu}{k}\right)\left(\frac{D}{L}\right)\right]^{1/3}\left(\frac{\mu}{\mu_s}\right)^{0.14}$		(6)
(2) For very long tubes				When $\left(\frac{GD}{\mu}\right)\left(\frac{c_p\mu}{k}\right)\left(\frac{D}{L}\right) < 20$, Eq. (6) should not be used		
(c) Annular spaces, turbulent flow All fluid properties at bulk temperature except μ_s at surface temperature t_s	McAdams	242	(9-32c)	$\frac{h}{c_p G}\left(\frac{c_p\mu}{k}\right)^{2/3}\left(\frac{\mu_s}{\mu}\right)^{0.14} = \frac{0.023}{(DeG/\mu)^{0.2}}$		(7)
II. Simplified equations for gases, turbulent flow inside tubes (Units are in lb_m, h, ft, °F, and Btu.)						
(a) Most common gases, turbulent flow (assuming $\mu = 0.0455$ lb_m/ft · h and $\mu c_p/k = 0.78$)	Obtained from Eq. (2)			$h = 0.0144(c_p G^{0.8}/D^{0.2})$		(8)
(b) Air at ordinary temperatures	Obtained from Eq. (2)			$h = c(G^{0.8}/D^{0.2})$	(See Note b)	(9)
(c) Fluorinated hydrocarbon refrigerant gas at ordinary pressures	Obtained from Eq. (2)			$h = c(G^{0.8}/D^{0.2})$	(See Note b)	(10)
(d) Ammonia gas at approximately 150°F, 300 psi	Obtained from Eq. (2)			$h = 0.00756(G^{0.8}/D^{0.2})$		(11)
At 0°F, 24 psi	Obtained from Eq. (2)			$h = 0.00604(G^{0.8}/D^{0.2})$		(12)
III. Simplified equations for liquids, turbulent flow inside tubes (Units are in lb_m, h, ft, °F, and Btu.)						
(a) Water at ordinary temperatures, 40 to 200°F. V is velocity in fps, D is tube ID in inches.	McAdams	228	(9-19)	$h = \frac{150(1 + 0.011t)V^{0.8}}{D^{0.2}}$		(13)
(b) Fluorinated hydrocarbon refrigerant liquid	Obtained from Eq. (2)			$h = c(G^{0.8}/D^{0.2})$	(See Note b)	(14)
(c) Ammonia liquid at approximately 100°F	Obtained from Eq. (2)			$h = 0.0156(G^{0.8}/D^{0.2})$		(15)
(d) Oil heating, approximate equation	Brown and Marco	146	(7-15)	$h = 0.034V/\mu_f^{0.63}$		(16)
(e) Oil cooling, approximate equation	Brown and Marco	146	(7-15)	$h = 0.0255V/\mu_f^{0.63}$		(17)
IV. Simplified equations for air						
(a) Vertical plane surfaces, V of 16 to 100 fps (room temperature)[c]	McAdams	249	(9-42)	$h' = 0.5V^{0.78}$		(18)
(b) Vertical plane surfaces, $V < 16$ fps (room temperature)[c]	McAdams	249	(9-42)	$h' = 0.99 + 0.21V$		(19)
(c) Single cylinder cross flow (film temperature = 200°F) $1000 < GD/\mu_f < 50{,}000$	McAdams	261	(10-3c)	$h = 0.026(G^{0.6}/D^{0.4})$		(20)
(d) Single sphere $17 < GD/\mu_f < 70{,}000$	McAdams	265	(10-6)	$h = 0.37\frac{k_f}{D}\left(\frac{GD}{\mu_f}\right)^{0.6}$		(21)
V. Gases flowing normal to pipes (dimensionless)						
(a) Single cylinder Re from 0.1 to 1000	McAdams	260	(10-3)	$\frac{hD}{k_f} = 0.32 + 0.43\left(\frac{GD}{\mu}\right)^{0.52}$		(22)
Re from 1000 to 50,000	McAdams	260	(10-3)	$\frac{hD}{k_f} = 0.24\left(\frac{GD}{\mu_f}\right)^{0.6}$		(23)
(b) Unbaffled staggered tubes, 10 rows. Approximate equation for turbulent flow[d]	McAdams	272	(10-11a)	$\frac{hD}{k_f} = 0.33\left(\frac{G_{max}D}{\mu_f}\right)^{0.6}\left(\frac{\mu c_p}{k}\right)_f^{1/3}$		(24)
(c) Unbaffled in-line tubes, 10 rows. Approximate equation for turbulent flow[d] ($G_{max}D/\mu_f$) from 2000 to 32,000	McAdams	272	(10-11a)	$\frac{hD}{k_f} = 0.26\left(\frac{G_{max}D}{\mu_f}\right)^{0.6}\left(\frac{\mu c_p}{k}\right)_f^{1/3}$		(25)

[a] McAdams (1954) recommends this equation for heating and cooling. Others recommend exponents of 0.4 for heating and 0.3 for cooling, with a change in constant.
[b] Table 7 in Chapter 2 of the 1981 *ASHRAE Handbook—Fundamentals* lists values for c.
[c] h' is expressed in Btu/h·ft²·°F based on initial temperature difference.
[d] G_{max} is based on *minimum* free area. Coefficients for tube banks depend greatly on geometrical details. These values approximate only.

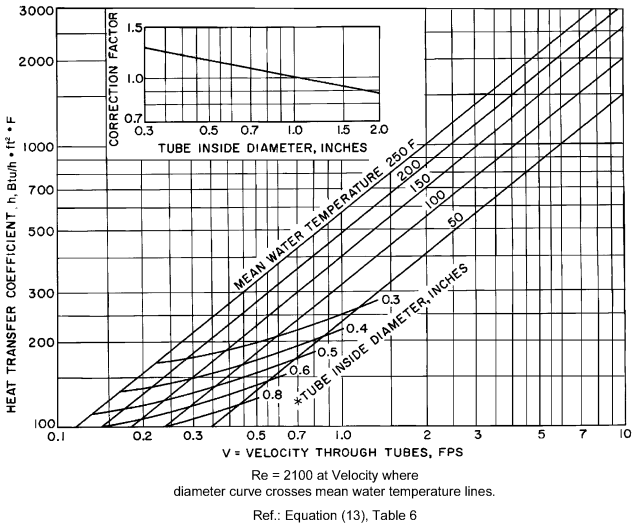

Fig. 11 Heat Transfer Coefficient for Turbulent Flow of Water Inside Tubes

The characteristic length D is the diameter of the tube, outside or inside, or the length of the plane plate. For other shapes, the hydraulic diameter D_h is used. With a uniform surface temperature and assuming uniform heat transfer coefficient the inlet and exit temperatures are related by:

$$D_h = 2r_h = 4 \times \frac{\text{Cross-sectional area for flow}}{\text{Total wetted perimeter}}$$

This reduces to twice the distance between surfaces for parallel plates or an annulus.

Simplified equations applicable to common fluids under normal operating conditions appear in Equations (8) through (25) of Table 6. Figure 11 gives graphical solutions for water. However, the value of the convective heat transfer coefficient with internal flows varies in the direction of the flow because of the temperature dependence of the properties of the fluids. In such a case a representative value of the heat transfer coefficient evaluated at the inlet and exit temperatures can be used in the above equation.

HEAT TRANSFER AUGMENTATION TECHNIQUES

As discussed by Bergles (1998), techniques applied to augment (enhance) heat transfer can be classified as passive methods, which require no direct application of external power, or as active schemes, which require external power. Examples of passive techniques include rough surfaces, extended surfaces, displaced promoters, and vortex flow devices. Examples of active techniques include mechanical aids, surface vibration, fluid vibration, and electrostatic fields. The effectiveness of a given augmentation technique depends largely on the mode of heat transfer or the type of heat exchanger to which it is applied.

When augmentation is used, the dominant thermal resistances in Equation (9) should be considered; that is, do not invest in reducing an already low thermal resistance (increasing an already high heat transfer coefficient). Additionally, heat exchangers with a large number of heat transfer units (NTU) show relatively small gains in effectiveness with augmentation [see Equations (24) and (26)]. Finally, the increased friction factor that usually accompanies the heat transfer augmentation must be considered.

Passive Techniques

Several examples of tubes with internal roughness or fins are shown in Figure 12. Rough surfaces of the spiral repeated rib variety are widely used to improve in-tube heat transfer with water, as in

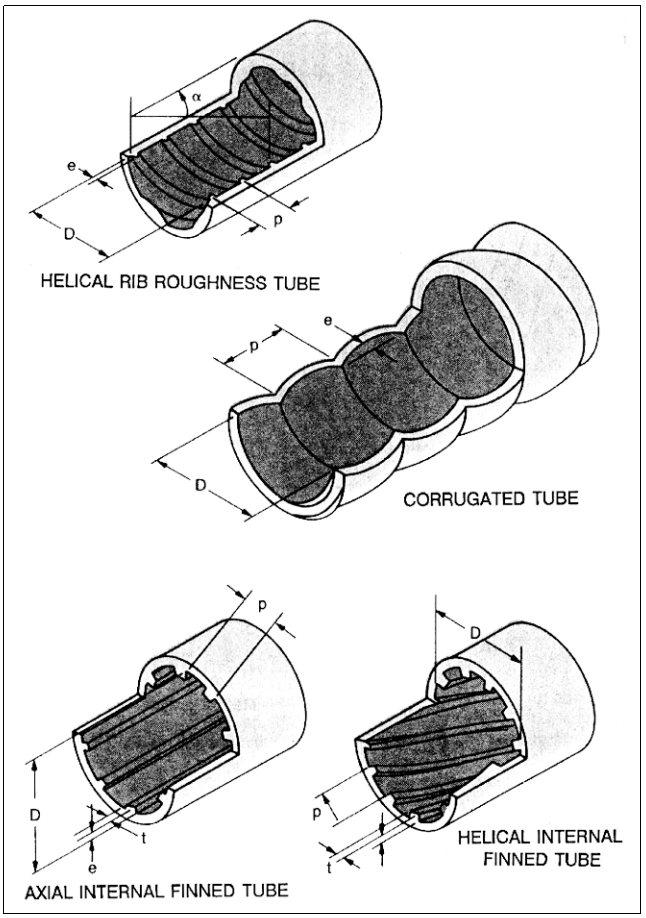

Fig. 12 Typical Tube-Side Enhancements

flooded chillers. The roughness may be produced by spirally indenting the outer wall, forming the inner wall, or inserting coils. Longitudinal or spiral internal fins in tubes can be produced by extrusion or forming and give a substantial increase in the surface area. The fin efficiency (see the section on Fin Efficiency on p. 3.20) can usually be taken as unity. Twisted strips (vortex flow devices) can be inserted as original equipment or as retrofit devices. From a practical point of view, the twisted tape width should be such that the tape can be easily inserted or removed. Ayub and Al-Fahed (1993) addressed the issue of the clearance between the twisted tape and tube inside dimension.

Microfin tubes (internally finned tubes with about 60 short fins around the circumference) are widely used in refrigerant evaporation and condensers. Since the gas entering the condenser in vapor-compression refrigeration is superheated, a considerable portion of the condenser acts to desuperheat the flow (i.e., it is single phase). Some data on the single-phase performance of microfin tubes, showing considerably higher heat transfer coefficients than for plain tubes, are available (e.g., Khanpara et al. 1986, Al-Fahed et al. 1993), but the upper Reynolds numbers of about 10,000 are lower than those found in practice. This deficiency is being addressed in a current ASHRAE research project.

The increased friction factor may not require increased pumping power if the flow rate can be adjusted or if the length of the heat exchanger can be reduced. Nelson and Bergles (1986) discuss this issue of performance evaluation criteria, especially for HVAC applications.

Of concern in chilled water systems is the fouling that in some cases may seriously reduce the overall heat transfer coefficient U. In general, fouled enhanced tubes perform better than fouled plain tubes,

as shown in studies of scaling due to cooling tower water (Knudsen and Roy 1983) and particulate fouling (Somerscales et al. 1991). A comprehensive review of fouling with enhanced surfaces is presented by Somerscales and Bergles (1997).

Fire-tube boilers are frequently fitted with **turbulators** to improve the turbulent convective heat transfer coefficient constituting the dominant thermal resistance. Also, due to the high gas temperatures, radiation from the convectively heated insert to the tube wall can represent as much as 50% of the total heat transfer. (Note, however, that the magnitude of the convective contribution decreases as the radiative contribution increases because of the reduced temperature difference.) Two commercial bent-strip inserts, a twisted-strip insert, and a simple bent-tab insert are depicted in Figure 13. Design equations, for convection only, are included in Table 7. Beckermann and Goldschmidt (1986) present procedures to include radiation, and Junkhan et al. (1985, 1988) give friction factor data and performance evaluations.

Several enhanced surfaces for gases are depicted in Figure 14. The offset strip fin is an example of an interrupted fin that is often found in compact plate fin heat exchangers used for heat recovery from exhaust air. Design equations are included in Table 7. These equations are comprehensive in that they apply to laminar and transitional flow as well as to turbulent flow, which is a necessary feature because the small hydraulic diameter of these surfaces drives the Reynolds number down. Data for other surfaces (wavy, spine, louvered, etc.) are given in the section on Bibliography.

Plastic heat exchangers have been suggested for HVAC applications (Pescod 1980) and are being manufactured for refrigerated sea water (RSW) applications. They could be made of materials impervious to corrosion, say from acidic condensate when cooling a gaseous stream (flue gas heat recovery), and could easily be manufactured with enhanced surfaces. Several companies now offer heat exchangers in plastic, including various enhancements.

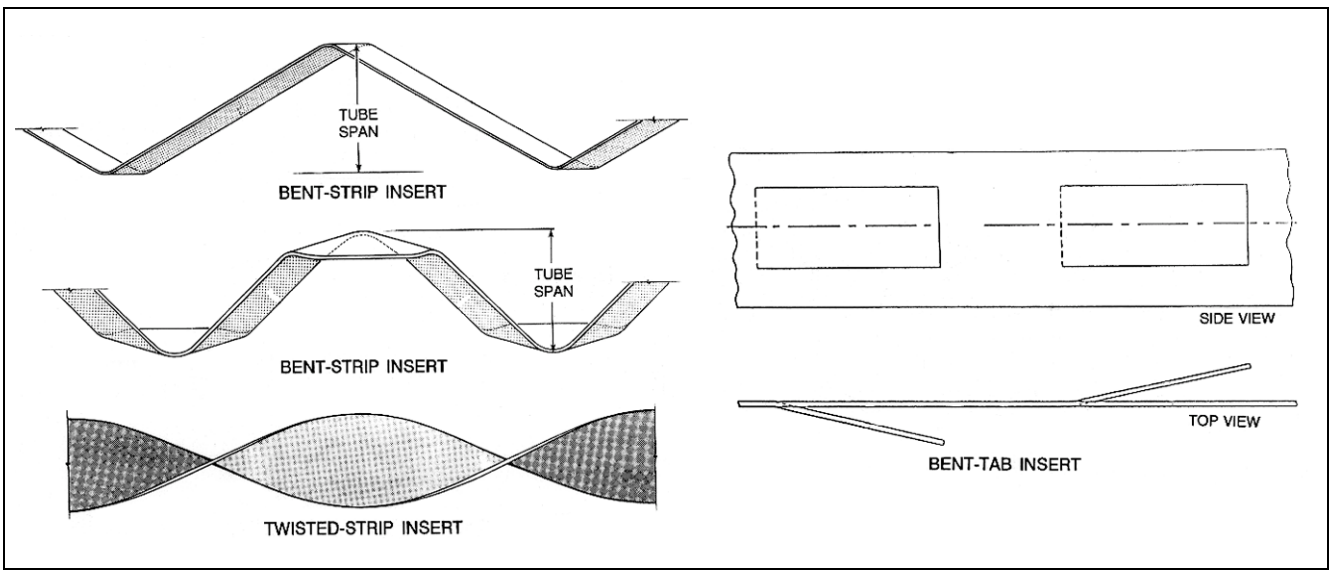

Fig. 13 Turbulators for Fire-Tube Boilers

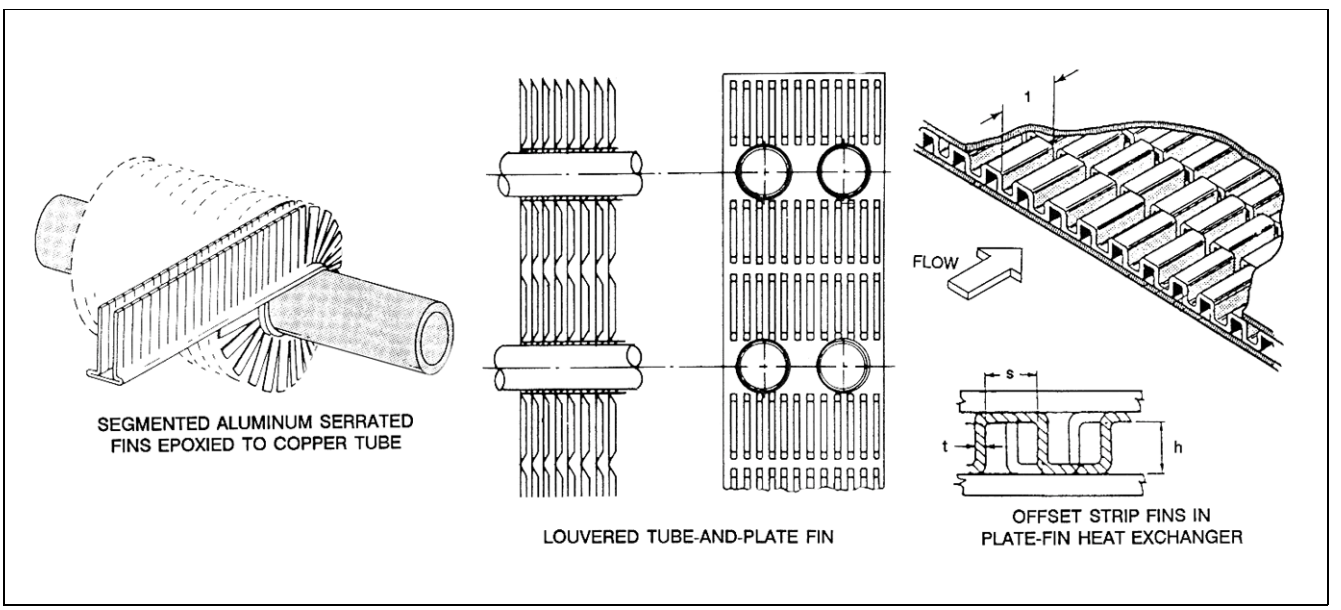

Fig. 14 Enhanced Surfaces for Gases

Table 7 Equations for Augmented Forced Convection (Single Phase)

Description	Equation
I. Turbulent in-tube flow of liquids	
(a) Spiral repeated rib[a]	$\frac{h_a}{h_s} = \left\{ \left[1 + 2.64 \left(\frac{GD}{\mu} \right)^{0.036} \left(\frac{e}{d} \right)^{0.212} \left(\frac{p}{d} \right)^{-0.21} \left(\frac{\alpha}{90} \right)^{0.29} \left(\frac{c_p \mu}{k} \right)^{-0.024} \right]^7 \right\}^{1/7}$
	$\frac{f_a}{f_s} = \left\{ 1 + \left[29.1 \left(\frac{GD}{\mu} \right)^{w} \left(\frac{e}{d} \right)^{x} \left(\frac{p}{d} \right)^{y} \left(\frac{\alpha}{90} \right)^{z} \left(1 + \frac{2.94}{n} \right) \sin \beta \right]^{15/16} \right\}^{16/15}$
	where
	$w = 0.67 - 0.06(p/d) - 0.49(\alpha/90)$
	$x = 0.37 - 0.157(p/d)$
	$y = -1.66 \times 10^{-6}(GD/\mu) - 0.33(\alpha/90)$
	$z = 4.59 + 4.11 \times 10^{-6}(GD/\mu) - 0.15(p/d)$
	$h_s = \frac{(k/D)(f_s/2)\left(\frac{GD}{\mu} \right)\left(\frac{c_p \mu}{k} \right)}{1 + 12.7(f_s/2)^{0.5}\left[\left(\frac{c_p \mu}{k} \right)^{2/3} - 1 \right]}$
	$f_s = \left[1.58 \ln \left(\frac{GD}{\mu} \right) - 3.28 \right]^{-2}$
(b) Fins[b]	$\frac{hD_h}{k} = 0.023 \left(\frac{c_p \mu}{k} \right)^{0.4} \left(\frac{GD_h}{\mu} \right)^{0.8} \left(\frac{A_F}{A_{Fi}} \right)^{0.1} \left(\frac{A_i}{A} \right)^{0.5} (\sec \alpha)^3$
	$f_h = 0.046 \left(\frac{GD_h}{\mu} \right)^{-0.2} \left(\frac{A_F}{A_{Fi}} \right)^{0.5} (\sec \alpha)^{0.75}$
	Note that in computing the Reynolds number for (b) and (c) there is allowance for the reduced cross-sectional area.
(c) Twisted-strip inserts[c]	$\left(\frac{hd}{k} \right) / \left(\frac{hd}{k} \right)_{y=\infty} = [1 + 0.769/y]$
	$\left(\frac{hd}{k} \right)_{y=\infty} = 0.023 \left(\frac{GD}{\mu} \right)^{0.8} \left(\frac{c_p \mu}{k} \right)^{0.4} \left(\frac{\pi}{\pi - 4\delta/d} \right)^{0.8} \left(\frac{\pi + 2 - 2\delta/d}{\pi - 4\delta/d} \right)^{0.2} \phi$
	where
	$\phi = (\mu_b/\mu_w)^n$
	$n = \begin{cases} 0.18 \text{ for liquid heating} \\ 0.30 \text{ for liquid cooling} \end{cases}$
	$f = \frac{0.0791}{(GD/\mu)^{0.25}} \left(\frac{\pi}{\pi - 4\delta/d} \right)^{1.75} \left(\frac{\pi + 2 - 2\delta/d}{\pi - 4\delta/d} \right)^{1.25} \left(1 + \frac{2.752}{y^{1.29}} \right)$
II. Turbulent in-tube flow of gases	
(a), (b) Bent-strip inserts[d]	$\frac{hD}{k} \left(\frac{T_w}{T_b} \right)^{0.45} = 0.258 \left(\frac{GD}{\mu} \right)^{0.6}$
	$\frac{hD}{k} \left(\frac{T_w}{T_b} \right)^{0.45} = 0.208 \left(\frac{GD}{\mu} \right)^{0.63}$
(c) Twisted-strip inserts[d]	$\frac{hD}{k} \left(\frac{T_w}{T_b} \right)^{0.45} = 0.122 \left(\frac{GD}{\mu} \right)^{0.65}$
(d) Bent-tab inserts[d]	$\frac{hD}{k} \left(\frac{T_w}{T_b} \right)^{0.45} = 0.406 \left(\frac{GD}{\mu} \right)^{0.54}$
	Note that in computing the Reynolds number there is no allowance for the flow blockage of the insert.
III. Offset strip fins for plate-fin heat exchangers[e]	$\frac{h}{c_p G} = 0.6522 \left(\frac{GD_h}{\mu} \right)^{-0.5403} \alpha^{-0.1541} \delta^{0.1499} \gamma^{-0.0678} \left[1 + 5.269 \times 10^{-5} \left(\frac{GD_h}{\mu} \right)^{1.340} \alpha^{0.504} \delta^{0.456} \gamma^{-1.055} \right]^{0.1}$
	$f_h = 9.6243 \left(\frac{GD_h}{\mu} \right)^{-0.7422} \alpha^{-0.1856} \delta^{-0.3053} \gamma^{-0.2659} \left[1 + 7.669 \times 10^{-8} \left(\frac{GD_h}{\mu} \right)^{4.429} \alpha^{0.920} \delta^{3.767} \gamma^{0.236} \right]^{0.1}$
	where h/c_pG, f_h, and GD_h/μ are based on the hydraulic diameter, given by
	$D_h = 4shl/[2(sl + hl + th) + ts]$

References:
[a]Ravigururajan and Bergles (1985)
[b]Carnavos (1979)
[c]Manglik and Bergles (1993)
[d]Junkhan et al. (1985)
[e]Manglik and Bergles (1990)

Table 8 Active Heat Transfer Augmentation Techniques and the Most Relevant Heat Transfer Modes

Technique	Heat Transfer Mode					
	Forced Convection (Gases)	Forced Convection (Liquids)	Boiling	Evaporation	Condensation	Mass Transfer
Mechanical aids	NA	B	C	C	NA	B
Surface vibration	B	B	B	B	B	A
Fluid vibration	C	B	B	B	D	B
Electrostatic/Electrohydrodynamic	B	B	A	A	A	A
Suction/Injection	C	B	NA	NA	B	B
Jet impingement	B	B	NA	B	NA	C
Rotation	C	C	A	A	A	A
Induced flow	B	B	NA	NA	NA	C

A = Most significant B = Significant C = Somewhat significant D = Not significant NA = Not believed to be applicable

Table 9 World-Wide Status of Active Techniques

Technique	Country or Countries
Mechanical aids	Universally used in selected applications
Surface vibration	USA; not significant
Fluid vibration	Sweden; mostly used for sonic cleaning
Electrostatic/Electrohydrodynamic	Japan, USA and UK; successful prototypes in operation in Japan
Other electrical methods	UK, France, and USA
Suction/Injection	No significant activity
Jet impingement	France and USA; high temperature units and aerospace applications
Rotation	US industry and R&D-based in UK
Induced flow	USA leader in the technology, particularly in combustion

Table 10 Selected Studies on Mechanical Aids, Suction, and Injection

Source	Process	Heat Transfer Surface	Fluid	Maximum α
Valencia et al. (1996)	Natural convection	Fin type tube	Air	0.5
Jeng et al. (1995)	Natural convection/Suction	Asymmetric isothermal wall	Air	1.4
Inagaki and Komori (1993)	Turbulent natural convection/Suction	Vertical plate	Air	1.8
Dhir et al. (1992)	Forced convection/Injection	Tube	Air	1.45
Duignan et al. (1993)	Forced convection/Film boiling	Horizontal plate	Air	2.0
Son and Dhir (1993)	Forced convection/Injection	Annuli	Air	1.85
Malhotra and Mujumdar (1991)	Water to bed/Stirring	Granular bed	Air	3.0
Aksan and Borak (1987)	Pool of water/Stirring	Tube coils	Water	1.7
Hagge and Junkhan (1975)	Forced convection/Scraping	Cylindrical wall	Air	11.0
Hu and Shen (1996)	Turbulent natural convection	Converging ribbed tube	Air	1.0

Active Techniques

Unlike the passive techniques, active techniques require use of external power to sustain the enhancement mechanism.

Table 8 provides a list of the more commonly known active heat transfer augmentation techniques and the corresponding heat transfer mode believed most applicable to the particular technique. A listing of the various active techniques and their world-wide status is given in Table 9. The rankings in Tables 8 and 9 are based on a comprehensive review of the pertinent literature (Ohadi et al. 1996). Table 9 shows that among the eight listed active techniques, the electrostatic/electrohydrodynamic and rotation appear to apply to almost all important heat transfer modes, at least from an enhancement applicability view point. The information in Table 9 suggests that aside from the mechanical aids technique, which is universally used for selected applications, most other active techniques have limited commercial use so far and are still in the development stage. However, the significant research progress in recent years is now promising expedited commercialization for some of the active techniques, such as the electrostatic/electrohydrodynamic (EHD) technique. The following is a brief summary of the enhancement techniques listed in Table 9.

Mechanical Aids. Augmentation by mechanical aids involves stirring the fluid by mechanical means, such as mixers, stirrers, or surface scrapers. Stirrers and mixers that scrape the surface are extensively used in the chemical processing of highly viscous fluids, such as the flow of highly viscous plastic with air. Heat exchangers that employ mechanical aids for enhancement are often called **mechanically assisted heat exchangers**. The surface scraping method is widely used for viscous liquids in the chemical processing industry and can be applied to duct flow of gases. Hagge and Junkhan (1974) reported tenfold improvement in heat transfer coefficient for laminar flow of air over a flat plate. Table 10 provides a listing of selected works on mechanical aids, suction, and injection.

Injection. This method involves supplying a gas to a flowing liquid through a porous heat transfer surface or injecting a fluid of a similar type upstream of the heat transfer test section. Injected bubbles produce an agitation similar to that of nucleate boiling. Gose et al. (1957) bubbled gas through sintered or drilled heated surfaces and found that the heat transfer coefficient increased 500% in laminar flow and about 50% in turbulent flow. Wayner and Bankoff (1965) demonstrated that the heat transfer coefficient could be increased by 150% if a porous block was placed on the surface to stabilize the flow of liquid toward the surface. Tauscher et al. (1970) demonstrated up to a five-fold increase in local heat transfer coefficients by injecting a similar fluid into a turbulent tube flow, but the effect dies out at a length-to-diameter ratio of 10.

Table 11 Selected Studies on Rotation

Source	Process	Heat Transfer Surface	Fluids	Rotation Speed, rpm	Max. α
Prakash and Zerle (1995)	Natural convection	Ribbed duct	Air	Given as a function	1.3
Mochizuki et al. (1994)	Natural convection	Serpentine duct	Air	Given as a function	3.0
Lan (1991)	Solidification	Vertical tube	Water	400	NA
McElhiney and Preckshot (1977)	External condensation	Horizontal tube	Steam	40	1.7
Nichol and Gacesa (1970)	External condensation	Vertical cylinder	Steam	2700	4.5
Astaf'ev and Baklastov (1970)	External condensation	Circular disc	Steam	2500	3.4
Tang and McDonald (1971)	Nucleate boiling	Horizontal heated circular cylinder	R-113	1400	<1.2
Marto and Gray (1971)	In-tube boiling	Vertical heated circular cylinder	Water	2660	1.6

NA = Not Available

Table 12 Selected Studies on EHD Technique

Source	Process	Heat Transfer Surface/Electrode	Fluid	P/Q, %	Max. α
Poulter and Allen (1986)	Internal flow	Tube/Wire	Aviation fuel-hexane	NA	20
Fernandez and Poulter(1987)	Internal flow	Tube/Wire	Transformer oil	NA	23
Ohadi et al. (1996)	Internal flow	Smooth surface/Rod	PAO (oil-based fluid)	1.2	3.2
Ohadi et al. (1991)	Internal flow	Tube/Wire	Air	15	3.2
Owsenek and Seyed-Yagoobi(1995)	Forced convection	Horizontal flat plate	Air	NA	25
Ohadi et al. (1995)	In-tube boiling	Microfin tube/Helical	R-134a	0.1	6.5
Ohadi et al. (1995)	In-tube condensation	Smooth tube/Rod wire	R-134a	0.1	7.0
Wawzyniak and Seyed-Yagoobi (1996)	External condensation	Enhanced and smooth tubes/ Circular rods	R-113	0.08	6.2
Seyed-Yagoobi et al. (1996)	Pool boiling	Horizontal tube/ Straight and circular wires	R-123	0.1	12.6

NA = Not Available; P = EHD Power; Q = Heat Exchanger Capacity

The practical application of injection appears to be rather limited because of difficulty of cost-effective supplying and removing of the injection fluid.

Suction. The suction method involves fluid removal through a porous heated surface leading to reduced heat/mass transfer resistance at the surface. Kinney (1968) and Kinney and Sparrow (1970) reported that applying suction at the surface increased heat transfer coefficients for laminar film and turbulent flows, respectively. For laminar film condensation, Antonir and Tamir (1977) and Lienhard and Dhir (1972) indicated that heat transfer coefficient can be improved by several hundred percent when film thickening is reduced by suction. Jeng et al. (1995) conducted experiments on a vertical parallel channel with asymmetric, isothermal walls. A porous wall segment was embedded into a segment of the test section wall, and enhancement occurred as the hot air was sucked from the channel. The local heat transfer coefficient increased with increasing porosity. The maximum heat transfer enhancement obtained was 140%.

Fluid or Surface Vibration. Fluid or surface vibrations are natural processes that occur in most heat exchangers; however, naturally occurring vibration is rarely factored into thermal design. Vibration equipment is expensive, and use of this technique for heat transfer enhancement does not have industrial applications at this stage of development. Vibrations of a wire in a forced convecting airflow enhanced the heat transfer to air up to 300% (Nesis et al. 1994), depending on the amplitude of vibrations and frequency. By using standing waves in a fluid, the input power was reduced by 75% compared with a fan that provides the same heat transfer rate (Woods 1992). Lower frequencies are preferable because they are less harmful to those who use this method of augmenting heat transfer.

Rotation. Rotation is a type of heat transfer enhancement that occurs naturally in rotating electrical machinery, gas turbine blades, and some other equipment. The rotating evaporator, the rotating heat pipe, the Higee distillation column, and the Rotex absorption cycle heat pump are typical examples of previous work in this area. In rotating evaporators, the rotation effectively distributes the liquid on the outside surface of the rotating surface. Rotation of the heat transfer surface also seems to be a promising method for effectively removing the condensate and decreasing liquid film thickness. Substantial increases in heat transfer coefficients have been demonstrated by using centrifugal force, which may be several times greater than the gravity force.

As shown in Table 11, the heat transfer enhancement obtained in the various studies varies from slight improvement up to 450%, depending on the system and rotation speed. The rotation technique is of particular interest for use in two-phase flows, particularly in boiling and condensation. It has been demonstrated that this technique is not effective in the gas-to-gas heat recovery mode in laminar flow, but its application is more likely in turbulent flow. High power consumption, sealing and vibration problems, moving parts, and the expensive equipment required for rotation are some drawbacks of the rotation technique.

Electrohydrodynamics. The electrohydrodynamic (EHD) enhancement of heat transfer refers to the coupling of an electric field with the fluid field in a dielectric fluid medium. The net effect is the production of secondary motions that destabilize the thermal boundary layer near the heat transfer surface, leading to heat transfer coefficients that are often an order of magnitude higher than those achievable by any of the conventional enhancement techniques. Among the various active augmentation techniques, EHD has benefited the most from substantial research in the past two decades in Japan, the United States, and the United Kingdom (Ohadi 1991). Its applicability for heat transfer enhancement in many applications has already been demonstrated, including for refrigeration/HVAC systems, process heat exchangers, waste heat recovery devices, cryogenics, aircraft environmental control systems, avionic cooling systems, and space thermal systems.

Selected work on EHD heat transfer enhancement is listed in Table 12. The work has involved studies on phase change processes as well as the indicated single-phase process. In fact, EHD-enhanced boiling and condensation have attracted the most attention from industrial and academic researchers.

The EHD effect is generally applied by placing wire or plate electrodes parallel and adjacent to the heat transfer surface. Figure 15 presents four electrode configurations for augmentation of forced-convection heat/mass transfer in-tube flows. A high-voltage, low-current electric field charges the electrode and establishes the electrical body force required to initiate and sustain augmentation.

When compared with other active techniques, a number of important advantages have contributed to the fast progress of the

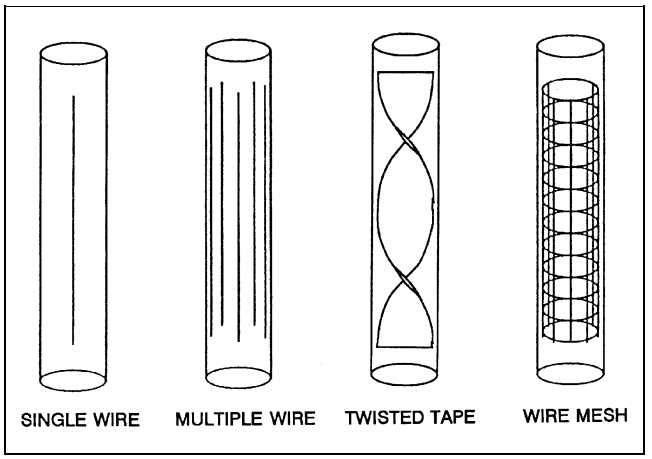

Fig. 15 Electrode Configurations for Internal Forced-Convection Flow

EHD technique in recent years. Rotation, injection, and vibration are generally mechanically complex and somewhat cumbersome to manufacture. Furthermore, the energy required to operate these systems can be a significant fraction of the power employed in pumping the fluid. In these respects, the EHD method of enhancement is superior.

The safety aspect of the EHD technique may be misjudged if careful attention is not paid to the manner in which these systems operate. Although EHD systems work at high voltages, the fact that very small currents are employed reduces the hazard of EHD fields to well below that of conventional low-voltage household appliances and ensures that the electrical power consumed by the EHD process is extremely small (less than 1% in most cases). Although the EHD technique appears to be well ahead of other active techniques, a number of issues remain to be addressed before successful implementation of this technique in practical heat exchangers can be realized. The most important issues include (1) any long-term effects the electric field may have on the heat exchanger, working fluid, and components, (2) the development of low-cost, high-voltage power supplies, and (3) identifying manufacturing processes that can lead to inexpensive mass production of EHD-enhanced heat exchangers. The encouraging news is that research work addressing some of the issues has already been initiated by researchers in the academic and government sectors and in private companies and research institutions. Additional details on the principles, applicability, and limitations of the EHD technique can be found elsewhere (Ohadi et al. 1991; Ohadi et al. 1999; Yabe 1991).

EXTENDED SURFACE

Heat transfer from a prime surface can be increased by attaching **fins** or **extended surfaces** to increase the area available for heat transfer. Fins provide a more compact heat exchanger with lower material costs for a given performance. To achieve optimum design, fins are generally located on the side of the heat exchanger where the heat transfer coefficients are low (such as the air side of an air-to-water coil). Equipment with an extended surface includes natural- and forced-convection coils and shell-and-tube evaporators and condensers. Fins are also used inside tubes in condensers and dry expansion evaporators.

Fin Efficiency

As heat flows from the root of a fin to its tip, temperature drops because of the thermal resistance of the fin material. The temperature difference between the fin and the surrounding fluid is therefore greater at the root than at the tip, causing a corresponding variation in the heat flux. Therefore, increases in fin length result in proportionately less additional heat transfer. To account for this effect, **fin efficiency** ϕ is defined as the ratio of the actual heat transferred from the fin to the heat that would be transferred if the entire fin were at its root or base temperature:

$$\phi = \frac{\int h(t - t_e)dA}{\int h(t_r - t_e)dA} \tag{50}$$

where ϕ is the fin efficiency, t_e is the temperature of the surrounding environment, and t_r is the temperature at the fin root. Fin efficiency is low for long fins, thin fins, or fins made of low thermal conductivity material. Fin efficiency decreases as the heat transfer coefficient increases because of the increased heat flow. For natural convection in air-cooled condensers and evaporators, where h for the air side is low, fins can be fairly large and fabricated from low-conductivity materials such as steel instead of from copper or aluminum. For condensing and boiling, where large heat transfer coefficients are involved, fins must be very short for optimum use of material.

The heat transfer from a finned surface, such as a tube, which includes both finned or secondary area A_s and unfinned or prime area A_p is given by the following equation:

$$q = (h_p A_p + \phi h_s A_s)(t_r - t_e) \tag{51}$$

Assuming the heat transfer coefficients for the finned surface and prime surface are equal, a *surface efficiency* ϕ_s can be derived for use in Equation (52).

$$\phi_s = 1 - \left(\frac{A_s}{A}\right)(1 - \phi) \tag{52}$$

$$q = \phi_s h A (t_r - t_e) \tag{53}$$

where A is the total surface area, equal to the sum of the finned and prime areas ($A = A_s + A_p$).

Temperature distribution and fin efficiencies for various fin shapes are derived in most heat transfer texts. Figures 16 through 19 show curves and equations for annular fins, straight fins, and spines. For constant thickness square fins, the efficiency of a constant thickness annular fin of the same area can be used. More accuracy, particularly with rectangular fins of large aspect ratio, can be obtained by dividing the fin into circular sectors (Rich 1966).

Rich (1966) presents results for a wide range of geometries in a compact form for equipment designers by defining a dimensionless thermal resistance Φ:

$$\Phi = \frac{R_f t_o k}{l^2} \tag{54}$$

$$R_f = \left(\frac{1}{h}\right)\left(\frac{1}{\phi} - 1\right) \tag{55}$$

where

Φ = dimensionless thermal resistance
ϕ = fin efficiency
t_o = fin thickness at fin base
l = length dimension = $r_t - r_o$ for annular fins
W = for rectangular fins

Rich (1966) also developed expressions for Φ_{max}, the maximum limiting value of Φ. Figure 20 gives Φ_{max} for annular fins of constant and tapered cross section as a function of $R = r_t/r_o$ (i.e., the

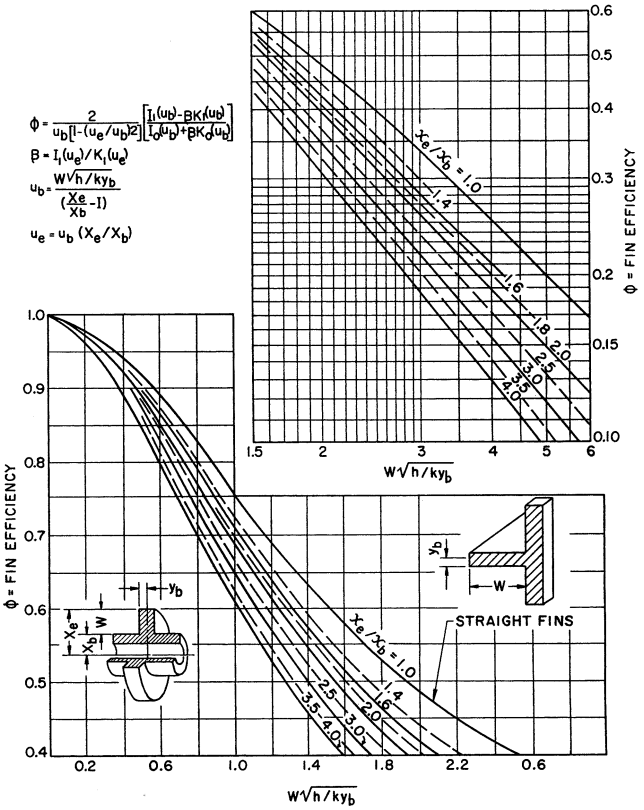

Fig. 16 Efficiency of Annular Fins of Constant Thickness

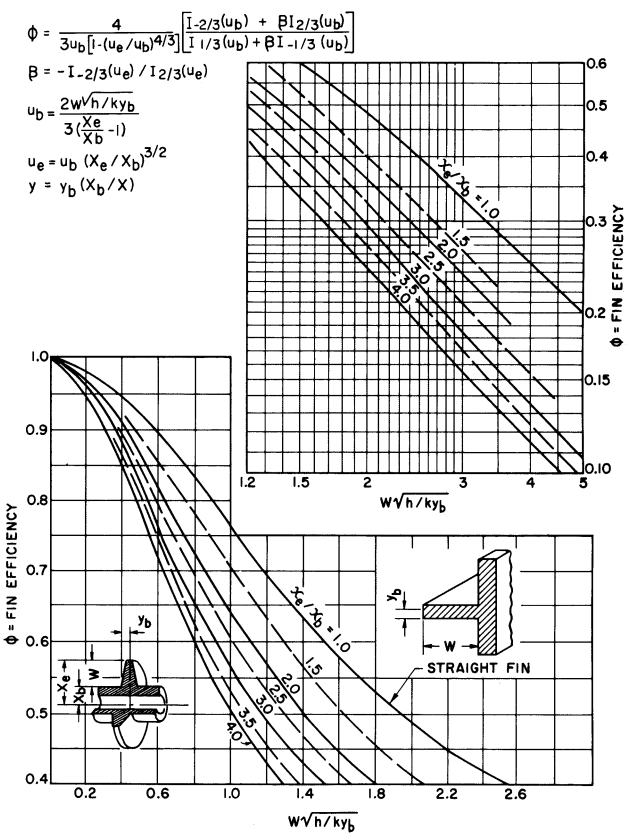

Fig. 17 Efficiency of Annular Fins with Constant Metal Area for Heat Flow

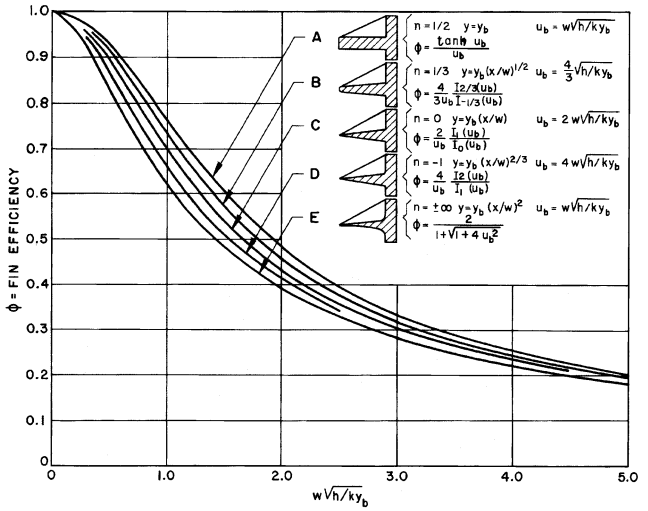

Fig. 18 Efficiency of Several Types of Straight Fin

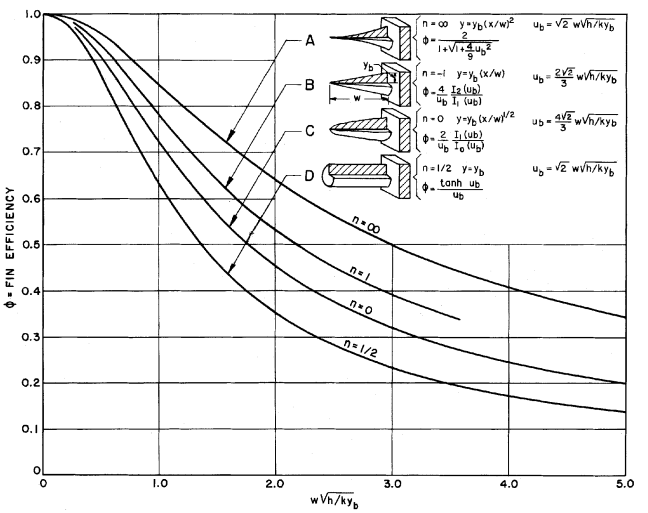

Fig. 19 Efficiency of Four Types of Spine

ratio of the fin tip-to-root radii). Figure 21 gives Φ_{max} for rectangular fins of a given geometry as determined by the sector method. Figure 22 gives correction factors (Φ/Φ_{max}) for the determination of Φ from Φ_{max} for both annular and rectangular fins.

Example. This example illustrates the use of the fin resistance for a rectangular fin typical of that for an air-conditioning coil.

Given: $L = 0.75$ in. $t_o = 0.006$ in.
$W = 0.50$ in. $h = 10$ Btu/h·ft^2·°F
$r_o = 0.25$ in. $k = 100$ Btu·ft/h·ft^2·°F

Solution: From Figure 18 at $W/r_o = 2.0$ and $L/W = 1.5$,

$$\Phi_{max} = R_{f(max)} t_o k / W^2 = 1.12$$

$$R_{f(max)} = \frac{1.12 \times 0.50^2}{0.006 \times 100 \times 12} = 0.0389 \text{ ft}^2 \cdot °\text{F} \cdot \text{h/Btu}$$

The correction factor Φ/Φ_{max}, which is multiplied by $R_{f(max)}$ to give R_f, is given in Figure 22 as a function of the fin efficiency. As a first approximation, the fin efficiency is calculated from Equation (54a) assuming $R_f = R_{f(max)}$.

$$\phi = 1/(1 + hR_f) \approx 0.72$$

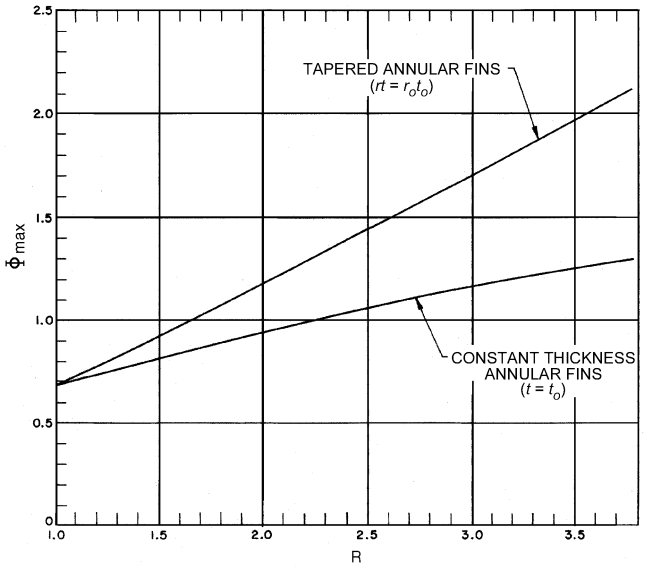

Fig. 20 Maximum Fin Resistance of Annular Fins
(Gardner 1945)

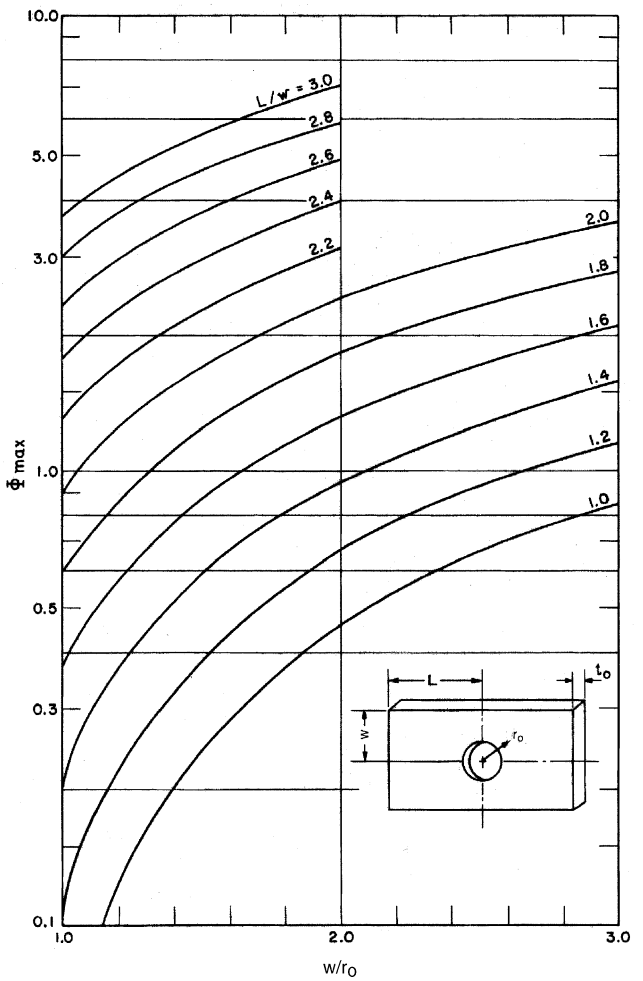

Fig. 21 Maximum Fin Resistance of Rectangular Fins Determined by Sector Method

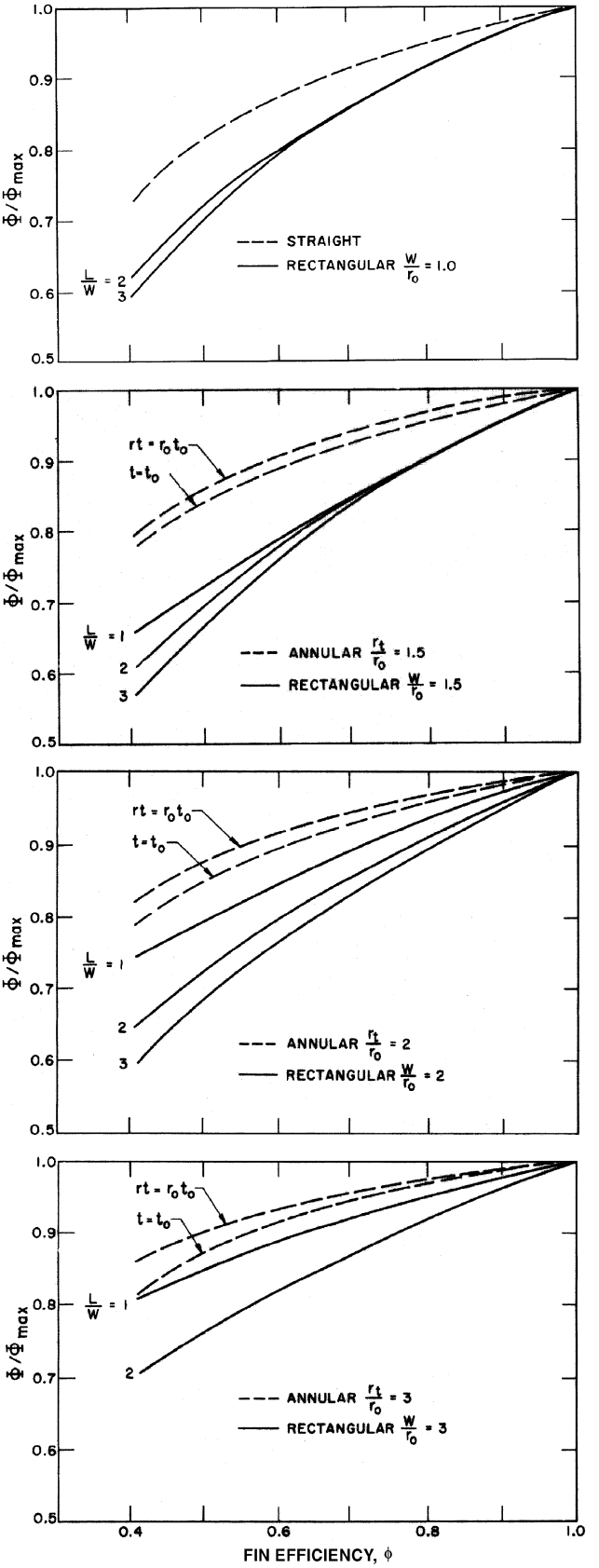

Fig. 22 Variation of Fin Resistance with Efficiency for Annular and Rectangular Fins
(Gardner 1945)

Interpolating between $L/W = 1$ and $L/W = 2$ at $W/r_o = 2$ gives

$$\Phi/\Phi_{max} = 0.88$$

Therefore,

$$R_f = 0.88 \times 0.0389 = 0.0342 \text{ ft}^2 \cdot °\text{F} \cdot \text{h/Btu}$$

The above steps may now be repeated using the corrected value of fin resistance.

$$\phi = 0.745$$
$$\Phi/\Phi_{max} = 0.90.75$$
$$R_f = 0.035 \text{ ft}^2 \cdot °\text{F} \cdot \text{h/Btu}$$

Note that the improvement in accuracy by reevaluating Φ/Φ_{max} is less than 1% of the overall thermal resistance (environment to fin base). The error produced by using $R_{f(max)}$ without correction is less than 3%. For many practical cases where greater accuracy is not warranted, a single value of R_f, obtained by estimating Φ/Φ_{max}, can be used over a range of heat transfer coefficients for a given fin. For approximate calculations, the fin resistance for other values of k and t_o can be obtained by simple proportion if the range covered is not excessive.

Schmidt (1949) presents approximate, but reasonably accurate, analytical expressions (for computer use) for circular, rectangular, and hexagonal fins. Hexagonal fins are the representative fin shape for the common staggered tube arrangement in finned-tube heat exchangers.

Schmidt's empirical solution is given by

$$\phi = \frac{\tanh(mr_i\Phi)}{mr_i\Phi}$$

where $m = \sqrt{2h/kt}$ and Φ is given by

$$\Phi = [(r_e/r_i) - 1][1 + 0.35\ln(r_e/r_i)]$$

For **circular fins**,

$$r_e/r_i = r_o/r_i$$

For **rectangular fins**,

$$r_e/r_i = 1.28\psi\sqrt{\beta - 0.2}, \quad \psi = M/r_i, \quad \beta = L/M \geq 1$$

where M and L are defined by Figure 23 as $a/2$ or $b/2$, depending on which is greater.

For **hexagonal fins**,

$$r_e/r_i = 1.27\psi\sqrt{\beta - 0.3}$$

where ψ and β are defined as above and M and L are defined by Figure 24 as $a/2$ or b (whichever is less) and $0.5\sqrt{(a^2/2)^2 + b^2}$, respectively.

The section on Bibliography lists other sources of information on finned surfaces.

Thermal Contact Resistance

Fins can be extruded from the prime surface (e.g., the short fins on the tubes in flooded evaporators or water-cooled condensers) or they can be fabricated separately, sometimes of a different material, and bonded to the prime surface. Metallurgical bonds are achieved by furnace-brazing, dip-brazing, or soldering. Nonmetallic bonding materials, such as epoxy resin, are also used. Mechanical bonds are obtained by tension-winding fins around tubes (spiral fins) or expanding the tubes into the fins (plate fins). Metallurgical bonding, properly done, leaves negligible thermal resistance at the joint but is not always economical. Thermal resistance of a mechanical bond

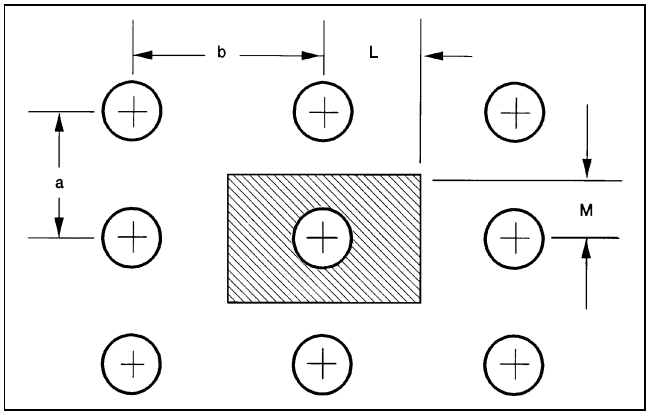

Fig. 23 Rectangular Tube Array

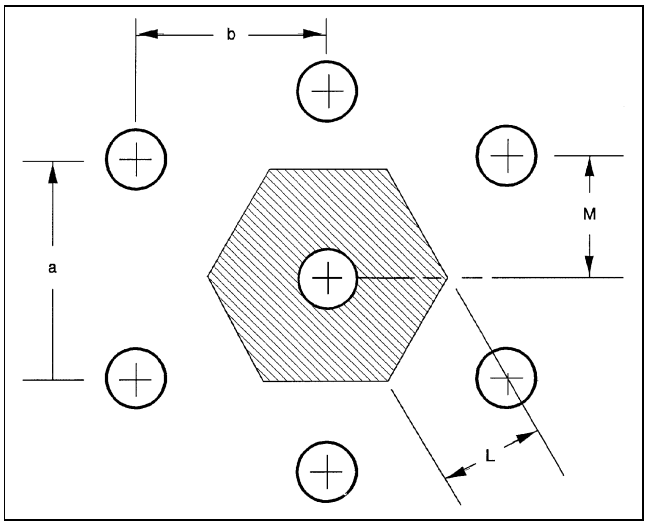

Fig. 24 Hexagonal Tube Array

may or may not be negligible, depending on the application, quality of manufacture, materials, and temperatures involved. Tests of plate fin coils with expanded tubes have indicated that substantial losses in performance can occur with fins that have cracked collars; but negligible thermal resistance was found in coils with continuous collars and properly expanded tubes (Dart 1959).

Thermal resistance at an interface between two solid materials is largely a function of the surface properties and characteristics of the solids, the contact pressure, and the fluid in the interface, if any. Eckels (1977) models the influence of fin density, fin thickness, and tube diameter on contact pressure and compared it to data for wet and dry coils. Shlykov (1964) shows that the range of attainable contact resistances is large. Sonokama (1964) presents data on the effects of contact pressure, surface roughness, hardness, void material, and the pressure of the gas in the voids. Lewis and Sauer (1965) show the resistance of adhesive bonds, and Kaspareck (1964) and Clausing (1964) give data on the contact resistance in a vacuum environment.

Finned-Tube Heat Transfer

The heat transfer coefficients for finned coils follow the basic equations of convection, condensation, and evaporation. The arrangement of the fins affects the values of constants and the exponential powers in the equations. It is generally necessary to refer to test data for the exact coefficients.

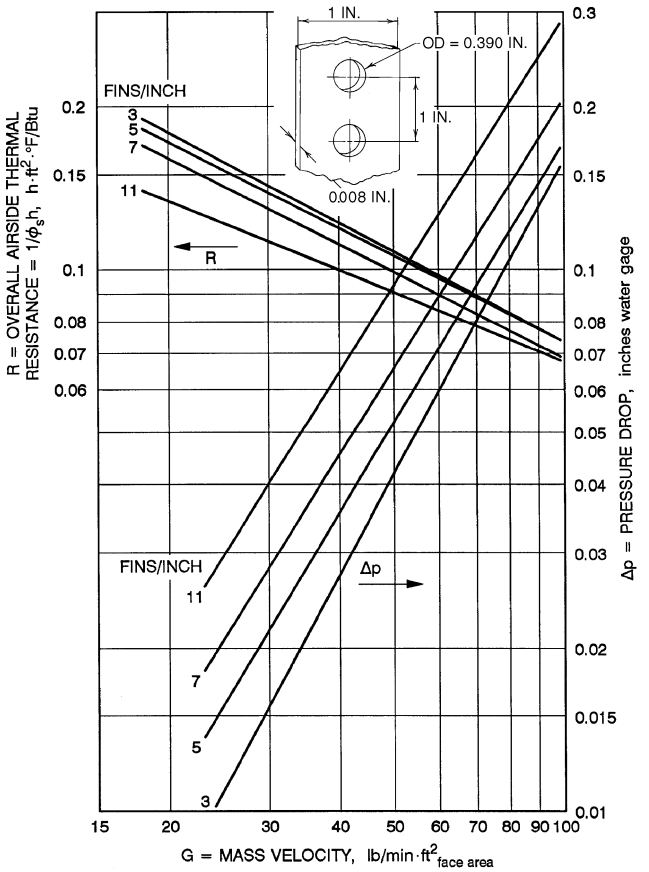

Fig. 25 Overall Air-Side Thermal Resistance and Pressure Drop for 1-Row Coils
(Shepherd 1946)

For natural-convection finned coils (gravity coils), approximate coefficients can be obtained by considering the coil to be made of tubular and vertical fin surfaces at different temperatures and then applying the natural-convection equations to each. This calculation is difficult because the natural-convection coefficient depends on the temperature difference, which varies at different points on the fin.

Fin efficiency should be high (80 to 90%) for optimum natural-convection heat transfer. A low fin efficiency reduces the temperature near the tip. This reduces Δt near the tip and also the coefficient h, which in natural convection depends on Δt. The coefficient of heat transfer also decreases as the fin spacing decreases because of interfering convection currents from adjacent fins and reduced free-flow passage; 2 to 4 in. spacing is common. Generally, high coefficients result from large temperature differences and small flow restriction.

Edwards and Chaddock (1963) give coefficients for several circular fin-on-tube arrangements, using fin spacing δ as the characteristic length and in the form $\mathrm{Nu} = f(\mathrm{Gr}\,\mathrm{Pr}\delta/D_o)$, where D_o is the fin diameter.

Forced-convection finned coils are used extensively in a wide variety of equipment. The fin efficiency for optimum performance is smaller than that for gravity coils because the forced-convection coefficient is almost independent of the temperature difference between the surface and the fluid. Very low fin efficiencies should be avoided because an inefficient surface gives a high (uneconomical) pressure drop. An efficiency of 70 to 90% is often used.

As fin spacing is decreased to obtain a large surface area for heat transfer, the coefficient generally increases because of higher air velocity between fins at the same face velocity and reduced equivalent diameter. The limit is reached when the boundary layer formed on one fin surface (Figure 8) begins to interfere with the boundary layer formed on the adjacent fin surface, resulting in a decrease of the heat transfer coefficient, which may offset the advantage of larger surface area.

Selection of the fin spacing for forced-convection finned coils usually depends on economic and practical considerations, such as fouling, frost formation, condensate drainage, cost, weight, and volume. Fins for conventional coils generally are spaced 14 to 6 per inch, except where factors such as frost formation necessitate wider spacing.

Several means are used to obtain higher coefficients with a given air velocity and surface, usually by creating air turbulence, generally with a higher pressure drop: (1) staggered tubes instead of in-line tubes for multiple-row coils; (2) artificial additional tubes, or collars or fingers made by suitably forming the fin materials; (3) corrugated fins instead of plane fins; and (4) louvered or interrupted fins.

Figure 25 shows data for one-row coils. The thermal resistances plotted include the temperature drop through the fins, based on one square foot of total external surface area.

The section on Bibliography lists other sources of information on fins.

SYMBOLS

A = surface area for heat transfer
A_F = cross-sectional flow area
C = conductance; or fluid capacity rate
C_1, C_2 = Planck's law constants [see Equation (33)]
c = coefficient or constant
c_p = specific heat at constant pressure
c_v = specific heat at constant volume
D = tube (inside) or rod diameter; or diameter of the vessel
d = diameter; or prefix meaning differential
E = electric field
e = emissivity; or protuberance height
F = angle factor [see Equations (40) and (41)]
Fo = Fourier number (see Table 1 and Figures 2, 3, and 4)
f = Fanning friction factor for single-phase flow; or electric body force
G = mass velocity; or irradiation
Gr = Grashof number
g = gravitational acceleration
h = heat transfer coefficient; or offset strip fin height
I = modified Bessel function
ID = inside diameter
J = mechanical equivalent of heat; or radiosity
j = heat transfer factor [see Equation (4), Table 6]
k = thermal conductivity
L = length; or height of liquid film
l = length; or length of one module of offset strip fins
M = mass; or molecular weight
m = general exponent
$\dot{m}$ = mass rate of flow
n = general number [see Equation (2) in Table 5 or Table 7 (c)]; or ratio r/r_m (see Figures 2, 3, and 4); or number of blades
NTU = number of exchanger heat transfer units [see Equation (17)]
Nu = Nusselt number
p = pressure; or fin pitch; or repeated rib pitch
Pr = Prandtl number
q = rate of heat transfer
q'' = heat flux
R = thermal resistance
Re = pipe Reynolds number (GD/μ); or film Reynolds number ($4\Gamma/\eta$)
Re* = rotary Reynolds number (D^2N_p/η)
r = radius
s = lateral spacing of offset fin strips
T = absolute temperature
t = temperature; or fin thickness at base
U = overall heat transfer coefficient
V = linear velocity
W = work; or total rate of energy emission; or fin dimension
W_λ = monochromatic emissive power
x, y, z = lengths along principal coordinate axes
Y = temperature ratio (see Figures 2, 3, and 4)

y = one-half diametrical pitch of a twisted tape: length of 180° revolution/tube diameter
Z = ratio of fluid capacity rates [see Equation (18)]
α = thermal diffusivity = $k/\rho c_p$ [Equation (28)]; or absorptance; or spiral angle for helical fins; or aspect ratio of offset strip fins, s/h; or enhancement factor: ratio of enhanced to unenhanced heat transfer coefficient—conditions remaining the same.
β = coefficient of thermal expansion; or contact angle of rib profile
Γ = mass flow of liquid per unit length
γ = ratio, t/s
Δ = difference between values
δ = distance between fins; or ratio t/l; or thickness of twisted tape
ε = hemispherical emittance; or exchanger heat transfer effectiveness [see Equation (16)]; or dielectric constant
λ = wavelength
μ = absolute viscosity
ν = kinematic viscosity
ρ = density; or reflectance
σ = Stefan-Boltzmann constant
τ = time; or transmittance [see Equation (39)]
Φ = fin resistance defined by Equation (54); Φ_{max} is maximum limiting value of Φ
ϕ = fin efficiency [see Equation (50)]; or angle [see Equation (41)]; or temperature correction factor [see Table 7(c)]

Subscripts

a = augmented
b = blackbody; or based on bulk fluid temperature
c = convection; or critical; or cold (fluid)
e = equivalent; or environment
f = film; or fin
fc = finite cylinder
frs = finite rectangular solid
g = gas
h = horizontal; or hot (fluid); or hydraulic
i = inlet; or inside; or particular surface (radiation); or based on maximum inside (envelope) diameter
ic = infinite cylinder
if = interface
is = infinite slab
iso = isothermal conditions
j = particular surface (radiation)
k = particular surface (radiation)
L = thickness
l = liquid
m = mean
max = maximum
min = minimum
n = counter variable
o = outside; or outlet; or overall; or at base of fin
p = prime heat transfer surface
r = radiation; or root (fin); or reduced
s = surface; or secondary heat transfer surface; or straight or plain; or accounting for flow blockage of twisted tape
st = static (pressure)
t = temperature; or terminal temperature; or tip (fin)
v = vapor; or vertical
w = wall; or wafer
λ = monochromatic
∞ = bulk

REFERENCES

Adams, J.A. and D.F. Rogers. 1973. *Computer aided heat transfer analysis*. McGraw-Hill, New York.

Afgan, N.H. and E.U. Schlunder. 1974. *Heat exchangers*: *Design and theory sourcebook*. McGraw-Hill, New York.

Aksan, D. and F. Borak. 1987. Heat transfer coefficients in coiled stirred tank systems. *Can. J. Chem. Eng*. 65:1013-14.

Al-Fahed, S.F., Z.H. Ayub, A.M. Al-Marafie, and B.M. Soliman. 1993. Heat transfer and pressure drop in a tube with internal microfins under turbulent water flow conditions. *Exp. Thermal and Fluid Science* 7:249-53.

Altmayer, E.F., A.J. Gadgil, F.S. Bauman, and R.C. Kammerud. 1983. Correlations for convective heat transfer from room surfaces. *ASHRAE Transactions* 89(2A):61-77.

Antonir, I. and A. Tamir. 1977. The effect of surface suction on condensation in the presence of a noncondensible gas. *International Journal of Heat and Mass Transfer* 99:496-99.

Astaf'ev, B.F. and A.M. Baklastov. 1970. Condensation of steam on a horizontal rotating disc. *Teploenergetika* 17:55-57.

Ayub, Z.H. and S.F. Al-Fahed. 1993. The effect of gap width between horizontal tube and twisted tape on the pressure drop in turbulent water flow, *International Journal of Heat and Fluid Flow* 14(1):64-67.

Bauman, F., A. Gadgil, R. Kammerud, E. Altmayer, and M. Nansteel. 1983. Convective heat transfer in buildings. *ASHRAE Transactions* 89(1A): 215-33.

Beckermann, C. and V. Goldschmidt. 1986. Heat transfer augmentation in the flueway of a water heater. *ASHRAE Transactions* 92(2B):485-95.

Bergles, A.E. 1998. Techniques to enhance heat transfer. In *Handbook of heat transfer,* 3rd ed., 11.1-11.76. McGraw-Hill, New York.

Brown, A.I. and S.M. Marco. 1958. *Introduction to heat transfer*, 3rd ed. McGraw-Hill, New York.

Burmeister, L.C. 1983. *Convective heat transfer*. John Wiley and Sons, New York.

Carnavos, T.C. 1979. Heat transfer performance of internally finned tubes in turbulent flow. In *Advances in enhanced heat transfer*, pp. 61-67. American Society of Mechanical Engineers, New York.

Carslaw, H.S. and J.C. Jaeger. 1959. *Conduction of heat in solids*. Oxford University Press, England.

Clausing, A.M. 1964. Thermal contact resistance in a vacuum environment. ASME *Paper* 64-HT-16, Seventh National Heat Transfer Conference.

Croft, D.R. and D.G. Lilley. 1977. *Heat transfer calculations using finite difference equations*. Applied Science Publishers, London.

Dart, D.M. 1959. Effect of fin bond on heat transfer. *ASHRAE Journal* 5:67.

Dhir, V.K., F. Chang, and G. Son. 1992. Enhancement of single-phase forced convection heat transfer in tubes and ducts using tangential flow injection. *Annual Report*. Contract No. 5087-260135. Gas Research Institute.

Duignan, M., G. Greene, and T. Irvine. 1993. The effect of surface gas injection on film boiling heat transfer. *Journal of Heat Transfer* 115:986-92.

Eckels, P.W. 1977. Contact conductance of mechanically expanded plate finned tube heat exchangers. AIChE-ASME Heat Transfer Conference, Salt Lake City, UT.

Edwards, J.A. and J.B. Chaddock. 1963. An experimental investigation of the radiation and free-convection heat transfer from a cylindrical disk extended surface. *ASHRAE Transactions* 69:313.

Fernandez, J. and R. Poulter. 1987. Radial mass flow in electrohydrodynamically-enhanced forced heat transfer in tubes. *International Journal of Heat and Mass Transfer* 80:2125-36.

Gardner, K.A. 1945. Efficiency of extended surface. *ASME Transactions* 67:621.

Gose, E.E., E.E. Peterson, and A. Acrivos. 1957. On the rate of heat transfer in liquids with gas injection through the boundary layer. *Journal of Applied Physics* 28:1509.

Grigull, U. et al. 1982. Heat transfer. *Proceedings of the Seventh International Heat Transfer Conference*, Munich 3. Hemisphere Publishing, New York.

Hagge, J.K. and G.H. Junkhan. 1974. Experimental study of a method of mechanical augmentation of convective heat transfer in air. *HTL3*, ISU-ERI-Ames-74158, Nov. 1975. Iowa State University, Ames, Iowa.

Hottel, H.C. and A.F. Sarofim. 1967. *Radiation transfer*. McGraw-Hill, New York.

Hu, Z. and J. Shen. 1996. Heat transfer enhancement in a converging passage with discrete ribs. *Int. J. Heat Mass Trans.* 39:1719.

Inagaki, T. and I. Komori. 1993. Experimental study of heat transfer enhancement in tubulent natural convection along a vertical flat plate, Part 1: The effect of injection and suction. *Heat Transactions—Japanese Research* 22:387.

Incropera, F.P. and D.P. DeWitt. 1996. *Fundamentals of heat transfer*. John Wiley and Sons, New York.

Jakob, M. 1949, 1957. *Heat transfer*, Vols. I and II. John Wiley and Sons, New York.

Jeng, Y., J. Chen, and W. Aung. 1995. Heat transfer enhancement in a vertical channel with asymmetric isothermal walls by local blowing or suction. *International Journal of Heat and Fluid Flow* 16:25.

Junkhan, G.H. et al. 1985. Investigation of turbulators for fire tube boilers. *Journal of Heat Transfer* 107:354-60.

Junkhan, G.H., A.E. Bergles, V. Nirmalan, and W. Hanno. 1988. Performance evaluation of the effects of a group of turbulator inserts on heat transfer from gases in tubes. *ASHRAE Transactions* 94(2):1195-1212.

Kaspareck, W.E. 1964. Measurement of thermal contact conductance between dissimilar metals in a vacuum. ASME *Paper* 64-HT-38, Seventh National Heat Transfer Conference.

Kays, W.M. and A.L. London. 1984. *Compact heat exchangers*, 3rd ed. McGraw-Hill, New York.

Kays, W.M. and M. Crawford. 1980. *Convective heat and mass transfer*, 2nd ed. McGraw-Hill, New York.

Khanpara, J.C., A.E. Bergles, and M.B. Pate. 1986. Augmentation of R-113 in-tube condensation with micro-fin tubes. HTD 65:21-32.

Kinney, R.B. 1968. Fully developed frictional and heat transfer characteristics of laminar flow in porous tubes. *International Journal of Heat and Mass Transfer* 11:1393-1401.

Kinney, R.B. and E.M. Sparrow. 1970. Turbulent flow: Heat transfer and mass transfer in a tube with surface suction. *Journal of Heat Transfer* 92:117-25.

Knudsen, J.G. and B.V. Roy. 1983. Studies on scaling of cooling tower water. *Fouling of heat enhancement surfaces*, pp. 517-30. Engineering Foundation, New York.

Lan, C.W. 1991. Effects of rotation on heat transfer fluid flow and interface in normal gravity floating zone crystal growth. *Journal of Crystal Growth* 114:517.

Lewis, D.M. and H.J. Sauer, Jr. 1965. The thermal resistance of adhesive bonds. ASME *Journal of Heat Transfer* 5:310.

Lienhard, J. and V.A. Dhir. 1972. Simple analysis of laminar film condensation with suction. *Journal of Heat Transfer* 94:334-36.

Malhotra, K. and A.S. Mujumdar. 1991. Wall to bed contact heat transfer rates in mechanically stirred granular beds. *International Journal of Heat and Mass Transfer* 34:724-35.

Manglik, R.M. and A.E. Bergles. 1990. The thermal-hydraulic design of the rectangular offset-strip-fin-compact heat exchanger. In *Compact heat exchangers*, pp. 123-49. Hemisphere Publishing, New York.

Manglik, R.M. and A.E. Bergles. 1993. Heat transfer and pressure drop correlation for twisted-tape insert in isothermal tubes: Part II —Transition and turbulent flows. *Journal of Heat Transfer* 115:890-96.

Marto, P.J. and V.H. Gray. 1971. Effects of high accelerations and heat fluxes on nucleate boiling of water in an axisymmetric rotating boiler. NASA *Technical Note* TN. D-6307. Washington, DC.

McAdams, W.H. 1954. *Heat transmission*, 3rd ed. McGraw-Hill, New York.

McElhiney, J.E. and G.W. Preckshot. 1977. Heat transfer in the entrance length of a horizontal rotating tube. *International Journal of Heat and Mass Transfer* 20:847-54.

Metais, B. and E.R.G. Eckert. 1964. Forced, mixed and free convection regimes. ASME *Journal of Heat Transfer* 86(C2)(5):295.

Mochizuki, S., J. Takamura, and S. Yamawaki. 1994. Heat transfer in serpentine flow passages with rotation. *J. Turbomachinery* 116:133.

Modest, M.F. 1993. *Radiation heat transfer*. McGraw-Hill, New York.

Myers, G.E. 1971. *Analytical methods in conduction heat transfer*. McGraw-Hill, New York.

Nelson, R.M. and A.E. Bergles. 1986. Performance evaluation for tubeside heat transfer enhancement of a flooded evaporative water chiller. *ASHRAE Transactions* 92(1B):739-55.

Nesis, E.I., A.F. Shatalov, and N.P. Karmatskii. 1994. Dependence of the heat transfer coefficient on the vibration amplitude and frequency of a vertical thin heater. *J. Eng. Physics and Thermophysics* 67(No. 1-2).

Nichol, A.A. and M. Gacesa. 1970. Condensation of steam on a rotating vertical cyclinder. *Journal of Heat Transfer* 144-52.

Ohadi, M.M. 1991. Heat transfer enhancement in heat exchangers. *ASHRAE Journal* (December):42-50.

Ohadi, M.M., S. Dessiatoun, A. Singh, K. Cheung, and M. Salehi. 1995a. EHD-Enhancement of boiling/condensation heat transfer of alternate refrigerants, *Progress Report* No. 6. Presented to the U.S. Department of Energy and the EHD Consortium Members, under DOE Grant No. DE-FG02-93CE23803.A000, Chicago, January 1995.

Ohadi, M.M., S.V. Dessiatoun, J. Darabi, and M. Salehi. 1996. Active augmentation of single-phase and phase-change heat transfer—An overview. In *Process enhanced and multiphase heat transfer: A festschrift for A.E. Bergles*, R.M. Manglik and A.D. Kraus, eds. Begell House Publishers, pp. 277-86.

Ohadi, M.M., J. Darabi, and B. Roget. 2000. Electrode design, materials, and fabrication fundamentals. In *Advances in Heat Transfer*,C.L. Tien, ed. Begell House Publishers.

Ohadi, M.M. et al. 1991. Electrohydrodynamic enhancement of heat transfer in a shell-and-tube heat exchanger. *Enhanced Heat Transfer* 4(1):19-39.

Ohadi, M.M., R. Papar, T.L. Ng, M. Faani, and R. Radermacher. 1992. EHD enhancement of shell-side boiling heat transfer coefficients of R-123/oil mixture. *ASHRAE Transactions* 98(2):427-34.

Owsenek, B. and J. Seyed-Yagoobi. 1995. Experimental investigation of corona wind heat transfer enhancement with a heated horizontal flat plate. *Journal of Heat Transfer* 117:309.

Parker, J.D., J.H. Boggs, and E.F. Blick. 1969. *Introduction to fluid mechanics and heat transfer*. Addison Wesley Publishing, Reading, MA.

Patankar, S.V. 1980. *Numerical heat transfer and fluid flow*. McGraw-Hill, New York.

Pescod, D. 1980. An advance in plate heat exchanger geometry giving increased heat transfer. HTD 10:73-77, American Society of Mechanical Engineers, New York.

Poulter, R. and P.H.G. Allen. 1986. Electrohydrodynamincally augmented heat and mass transfer in the shell tube heat exchanger. *Proceedings of the Eighth International Heat Transfer Conference* 6:2963-68.

Prakash, C. and R. Zerle. 1995. Prediction of turbulent flow and heat transfer in a ribbed rectangular duct with and without rotation. *J. Turbomachinery* 117:255.

Ravigururajan, T.S. and A.E. Bergles. 1985. General correlations for pressure drop and heat transfer for single-phase turbulent flow in internally ribbed tubes. *Augmentation of heat transfer in energy systems*, 52:9-20. American Society of Mechanical Engineers, New York.

Rich, D.G. 1966. The efficiency and thermal resistance of annular and rectangular fins. *Proceedings of the Third International Heat Transfer Conference*, AIChE 111:281-89.

Schmidt, T.E. 1949. Heat transfer calculations for extended surfaces. *Refrigerating Engineering* 4:351-57.

Schneider, P.J. 1964. *Temperature response charts*. John Wiley and Sons, New York.

Seyed-Yagoobi, J., C.A. Geppert, and L.M. Geppert. 1996. Electrohydrodynamically enhanced heat transfer in pool boiling. *ASME Journal of Heat Transfer* 118:233-37.

Shepherd, D.G. 1946. Performance of one-row tube coils with thin plate fins, low velocity forced convection. *Heating, Piping, and Air Conditioning* (April).

Shlykov, Y.P. 1964. Thermal resistance of metallic contacts. *International Journal of Heat and Mass Transfer* 7(8):921.

Siegel, R. and J.R. Howell. 1981. *Thermal radiation heat transfer*. McGraw-Hill, New York.

Somerscales, E.F.C. et al. 1991. Particulate fouling of heat transfer tubes enhanced on their inner surface. *Fouling and enhancement interactions*. HTD 164:17-28. American Society of Mechanical Engineers, New York.

Somerscales, E.F.C. and A.E. Bergles. 1997. Enhancement of heat transfer and fouling mitigation. *Advances in Heat Transfer* 30:197-253. Academic Press, San Diego.

Son, G. and V.K. Dhir. 1993. Enhancement of heat transfer in annulus using tangential flow injection. HTD-Vol. 246, *Heat Transfer in Turbulent Flows*, ASME.

Sonokama, K. 1964. Contact thermal resistance. *Journal of the Japan Society of Mechanical Engineers* 63(505):240. English translation in RSIC-215, AD-443429.

Sunada, K., A. Yabe, T. Taketani, and Y. Yoshizawa. 1991. Experimental study of EHD pseudo-dropwise condensation. *Proceedings of the ASME-JSME Thermal Engineering Joint Conference* 3:47-53.

Tang, S. and T.W. McDonald. 1971. A study of boiling heat transfer from a rotating horizontal cylinder. *International Journal of Heat and Mass Transfer* 14:1643-57.

Tauscher, W.A., E.M. Sparrow, and J.R. Lloyd. 1970. Amplification of heat transfer by local injection of fluid into a turbulent tube flow. *International Journal of Heat and Mass Transfer* 13*:*681-88.

Uemura, M., S. Nishio, and I. Tanasawa. 1990. Enhancement of pool boiling heat transfer by static electric field. *Ninth International Heat Transfer Conference*, 75-80.

Valencia, A., M. Fiebig, and V.K. Mitra. 1996. Heat transfer enhancement by longitudinal vortices in a fin tube heat exchanger. *Journal of Heat Transfer* 118:209.

Wawzyniak, M. and J. Seyed-Yagoobi. 1996. Augmentation of condensation heat transfer with electrohydrodynamics on vertical enhanced tubes. *ASME Journal of Heat Transfer* 118:499-502.

Wayner, P.C., Jr. and S.G. Bankoff. 1965. Film boiling of nitrogen with suction on an electrically heated porous plate. *AIChE Journal* 11:59-64.

Woods, B.G. 1992. Sonically enhanced heat transfer from a cylinder in cross flow and its impact on process power consumption. *International Journal of Heat and Mass Transfer* 35:2367-76.

Yabe, A. and H. Maki. 1988. Augmentation of convective and boiling heat transfer by applying an electrohydrodynamical liquid jet. *International Journal of Heat Mass Transfer* 31(2):407-17.

BIBLIOGRAPHY

Fins

General

Gunter, A.Y. and A.W. Shaw. 1945. A general correlation of friction factors for various types of surfaces in cross flow. *ASME Transactions* 11:643.

Shah, R.K. and R.L. Webb. 1981. *Compact and enhanced heat exchangers, heat exchangers, theory and practice*, pp. 425-68. J. Taborek et al., eds. Hemisphere Publishing, New York.

Webb, R.L. 1980. Air-side heat transfer in finned tube heat exchangers. *Heat Transfer Engineering* 1(3):33-49.

Smooth

Clarke, L. and R.E. Winston. 1955. Calculation of finside coefficients in longitudinal finned heat exchangers. *Chemical Engineering Progress* 3:147.

Elmahdy, A.H. and R.C. Biggs. 1979. Finned tube heat exchanger: Correlation of dry surface heat transfer data. *ASHRAE Transactions* 85:2.

Ghai, M.L. 1951. Heat transfer in straight fins. General discussion on heat transfer. London Conference, September.

Gray, D.L. and R.L. Webb. 1986. Heat transfer and friction correlations for plate finned-tube heat exchangers having plain fins. Proceedings of Eighth International Heat Transfer Conference, San Francisco.

Wavy

Beecher, D.T. and T.J. Fagan. 1987. Fin patternization effects in plate finned tube heat exchangers. *ASHRAE Transactions* 93:2.

Yashu, T. 1972. Transient testing technique for heat exchanger fin. *Reito* 47(531):23-29.

Spine

Abbott, R.W., R.H. Norris, and W.A. Spofford. 1980. Compact heat exchangers for General Electric products—Sixty years of advances in design and manufacturing technologies. *Compact heat exchangers—History, technological advancement and mechanical design problems*. R.K. Shah, C.F. McDonald, and C.P. Howard, eds. Book No. G00183, pp. 37-55. American Society of Mechanical Engineers, New York.

Moore, F.K. 1975. Analysis of large dry cooling towers with spine-fin heat exchanger elements. ASME *Paper* No. 75-WA/HT-46.

Rabas, T.J. and P.W. Eckels. 1975. Heat transfer and pressure drop performance of segmented surface tube bundles. ASME *Paper* No. 75-HT-45.

Weierman, C. 1976. Correlations ease the selection of finned tubes. *Oil and Gas Journal* 9:94-100.

Louvered

Hosoda, T. et al. 1977. Louver fin type heat exchangers. *Heat Transfer Japanese Research* 6(2):69-77.

Mahaymam, W. and L.P. Xu. 1983. Enhanced fins for air-cooled heat exchangers—Heat transfer and friction factor correlations. Y. Mori and W. Yang, eds. Proceedings of the ASME-JSME Thermal Engineering Joint Conference, Hawaii.

Senshu, T. et al. 1979. Surface heat transfer coefficient of fins utilized in air-cooled heat exchangers. *Reito* 54(615):11-17.

Circular

Jameson, S.L. 1945. Tube spacing in finned tube banks. *ASME Transactions* 11:633.

Katz, D.L. 1954-55. Finned tubes in heat exchangers; Cooling liquids with finned coils; Condensing vapors on finned coils; and Boiling outside finned tubes. Bulletin reprinted from *Petroleum Refiner.*

Heat Exchangers

Gartner, J.R. and H.L. Harrison. 1963. Frequency response transfer functions for a tube in crossflow. *ASHRAE Transactions* 69:323.

Gartner, J.R. and H.L. Harrison. 1965. Dynamic characteristics of water-to-air crossflow heat exchangers. *ASHRAE Transactions* 71:212.

McQuiston, F.C. 1981. Finned tube heat exchangers: State of the art for the air side. *ASHRAE Transactions* 87:1.

Myers, G.E., J.W. Mitchell, and R. Nagaoka. 1965. A method of estimating crossflow heat exchanger transients. *ASHRAE Transactions* 71:225.

Stermole, F.J. and M.H. Carson. 1964. Dynamics of forced flow distributed parameter heat exchangers. *AIChE Journal* 10(5):9.

Thomasson, R.K. 1964. Frequency response of linear counterflow heat exchangers. *Journal of Mechanical Engineering Science* 6(1):3.

Wyngaard, J.C. and F.W. Schmidt. Comparison of methods for determining transient response of shell and tube heat exchangers. ASME *Paper* 64-WA/HT-20

Yang, W.J. Frequency response of multipass shell and tube heat exchangers to timewise variant flow perturbance. ASME *Paper* 64-HT-18.

Heat Transfer, General

Bennet, C.O. and J.E. Myers. 1984. *Momentum, heat and mass transfer*, 3rd ed. McGraw-Hill, New York.

Chapman, A.J. 1981. *Heat transfer*, 4th ed. Macmillan, New York.

Holman, J.D. 1981. *Heat transfer*, 5th ed. McGraw-Hill, New York.

Kern, D.Q. and A.D. Kraus. 1972. *Extended surface heat transfer*. McGraw-Hill, New York.

Kreith, F. and W.Z. Black. 1980. *Basic heat transfer*. Harper and Row, New York.

Lienhard, J.H. 1981. *A heat transfer textbook*. Prentice Hall, Englewood Cliffs, NJ.

McQuiston, F.C. and J.D. Parker. 1988. *Heating, ventilating and air-conditioning, analysis and design*, 4th ed. John Wiley and Sons, New York.

Rohsenow, W.M. and J.P. Hartnett, eds. 1973. *Handbook of heat transfer.* McGraw-Hill, New York.

Sissom, L.E. and D.R. Pitts. 1972. *Elements of transport phenomena*. McGraw-Hill, New York.

Smith, E.M. 1997. *Thermal design of heat exchangers.* John Wiley and Sons, Chichester, UK.

Todd, J.P. and H.B. Ellis. 1982. *Applied heat transfer*. Harper and Row, New York.

Webb, R.L. and A.E. Bergles. 1983. Heat transfer enhancement, second generation technology. *Mechanical Engineering* 6:60-67.

Welty, J.R. 1974. *Engineering heat transfer*. John Wiley and Sons, New York.

Welty, J.R., C.E. Wicks, and R.E. Wilson. 1972. *Fundamentals of momentum, heat and mass transfer*. John Wiley and Sons, New York.

Wolf, H. 1983. *Heat transfer.* Harper and Row, New York.